Nordic nuclear safety research

NKS-414
ISBN 978-87-7893-503-8

Activity estimation of shielded or hidden radionuclides in emergency conditions: Impact of environmental conditions

[1]H. Toivonen
[2]H. Ramebäck
[2]M. Granström
[1]S. Ihantola
[3]G. Jónsson
[3]M. Ilkov
[4]M. Kilkki

[1]HT Nuclear, Finland
[2]FOI, Sweden
[3]IRSA, Iceland
[4]Environics, Finland

December 2018

Abstract

In 2017 an NKS project focused on the shield analysis, which showed that the spectrum contains enough information to determine the attenuation of the photons in a material between the source and the detector. Two approaches were studied: the step ratio- and the peak ratio methods. In the step ratio method, the height of the step just below a full energy peak originates from photon scattering to small angles, primarily from scattering in a shield. Using that information, the ratio of the step divided by the net area of the peak, is a function of the shield thickness. If a calibration is done with different thicknesses, that calibration can be used to determine the shield thickness. Moreover, with knowledge of the distance between the detector and the source and the efficiency of the detector at a reference distance, the activity of the source can be determined. The other approach, the peak ratio method, can be used for radionuclides emitting more than one gamma photon having enough difference in energies in its decay. That method uses the fact that the attenuation of the two gamma rays will be different. Again, knowledge of the distance and the efficiency of the detector gives the source activity.

The study in 2017 showed the effect of the environment on the shield analysis for the step ratio method when the information in the step just below a peak is to be used for the analysis. The present study focuses on the impact of the environment for this method. In particular, material other than the shield, including the ground, contributes to the small angle scattering and therefore to the step underneath the peaks. Such contributions will cause a bias in the method which has to be accounted for in the uncertainty calculation.

Another problem correlated to the uncertainty estimation is the fact that the activity of a shielded source is not linear with respect to some input quantities. If the uncertainty of those input quantities is large, normal uncertainty propagation will result in bad estimates for the uncertainty. One solution to this problem is to apply a Monte Carlo method, i.e. propagate the distributions. This was also done for the activity estimations in this work.

Key words

Gamma spectrometry, radioactive sources, activity determination, shielded sources, nuclear security

NKS-414
ISBN 978-87-7893-503-8
Electronic report, December 2018
NKS Secretariat
P.O. Box 49
DK - 4000 Roskilde, Denmark
Phone +45 4677 4041
www.nks.org
e-mail nks@nks.org

RadShield2

Harri Toivonen (FIN), Henrik Ramebäck (SWE), Micael Granström (SWE),

Sakari Ihantola (FIN), Gísli Jónsson (ISL), Marjan Ilkov (ISL), Mikko Kilkki (FIN)

Activity estimation of shielded or hidden radionuclides in emergency conditions: Impact of environmental conditions

RadShield2

NKS project 2018

Coordinator:

Swedish Defence Research Agency, FOI (SE)

Henrik Ramebäck

Participants:

Swedish Defence Research Agency (SWE)

Micael Granström

Henrik Ramebäck

HT Nuclear (FIN)

Harri Toivonen

Sakari Ihantola

Icelandic Radiation Safety Authority (ISL)

Gisli Jonsson

Marjan Ilkov

DTU Nutech (DEN)

N. Markovic

Environics Oy (FIN)

Mikko Kilkki

NRPA (NOR)

Bredo Møller

Measurements:

Micael Granström (SWE), Harri Toivonen (FIN), Sakari Ihantola (FIN), Gísli Jónsson (ISL), Marjan Ilkov (ISL) Henrik Ramebäck (SWE), Mikko Kilkki (FIN)

Observers:

Jake Livesay (IB3 Global Solutions, USA), Ahti Luukkonen (Environics, FIN)

Abstract

In order to perform a threat assessment related to the properties of an unknown radioactive source, the following tasks need to be addressed: detection of the source, identification of the radionuclides involved, source localization, and activity determination based on a shield analysis around the source (attenuation).

In 2017 an NKS project focused on the shield analysis, which showed that the spectrum contains enough information to determine the attenuation of the photons in a material between the source and the detector. Two approaches were studied: the step ratio- and the peak ratio methods. In the step ratio method, the height of the step just below a full energy peak originates from photon scattering to small angles, primarily from scattering in a shield. Using that information, the ratio of the step divided by the net area of the peak, is a function of the shield thickness. If a calibration is done with different thicknesses, that calibration can be used to determine the shield thickness. Moreover, with knowledge of the distance between the detector and the source and the efficiency of the detector at a reference distance, the activity of the source can be determined. The other approach, the peak ratio method, can be used for radionuclides emitting more than one gamma photon having enough difference in energies in its decay. That method uses the fact that the attenuation of the two gamma rays will be different. Again, knowledge of the distance and the efficiency of the detector gives the source activity.

The study in 2017 showed the effect of the environment on the shield analysis for the step ratio method when the information in the step just below a peak is to be used for the analysis. The present study focuses on the impact of the environment for this method. In particular, material other than the shield, including the ground, contributes to the small angle scattering and therefore to the step underneath the peaks. Such contributions will cause a bias in the method which has to be accounted for in the uncertainty calculation.

Another problem correlated to the uncertainty estimation is the fact that the activity of a shielded source is not linear with respect to some input quantities. If the uncertainty of those input quantities is large, normal uncertainty propagation will result in bad estimates for the uncertainty. One solution to this problem is to apply a Monte Carlo method, i.e. propagate the distributions. This was also done for the activity estimations in this work.

Key words

Gamma spectrometry, radioactive sources, activity determination, shielded sources, nuclear security

1. Introduction

Measurement of radioactive and nuclear material is important in e.g. environmental monitoring, treaty verification and in nuclear security. One critical characteristic during a nuclear security event involving a radioactive source is the activity, since it will determine the potential consequences of the event. Activity measurement methods of e.g. gamma emitting radionuclides in laboratories are well-established, but in the field it might become more difficult due to e.g. environmental conditions and shielding. Heavily shielded sources might from a measurement point-of-view look innocent since the signal in a detector will be small even for a very strong source. However, a measured spectrum will contain information about possible shielding. By analysing the spectrum the thickness of a shield can be estimated and furthermore the activity of the source. In one approach in the present study the ratio of two peaks from one radionuclide is used in order to determine the shield thickness and the activity since the attenuation will differ for the two gamma energies. Another approach uses the information, i.e. the step, beneath the peak of e.g. a single photon emitter since the step ratio is dependent on the magnitude of the scattering of the gamma photons.

In 2017 an NKS funded project to evaluate the possibilities to measure the activity of shielded sources was initiated. One of the key conclusions from that project was that the environment seemed to influence the precision of the measurements, in particular for the step ratio method. The rationale for the continuation of the project was to evaluate the influence of environmental factors in order to achieve a better uncertainty estimation of the measured activity.

2. Step ratio (SR) for shielding analysis

2.1 Compton scattering to small angles

The simulations in the previous RadShield project 2017 [NKS-399] showed that the step on the left side of a full energy peak is caused by Compton scattering into small angles. For ^{137}Cs, the simulations revealed that the spectral counts less than 10 keV below the full energy peak are caused by scattering into angles smaller than 10 degrees. This can be verified from the well-known equation of Compton scattering:

$$E' = \frac{1}{1/E_0[1-\cos(\theta)]+1/E} \quad (2.1)$$

With a peak energy of E =661 keV, the electron rest mass (E_0=511 keV) and maximum scatter angle (θ=10^0), the energy of the scattered gamma-rays E' = 649 keV. Scattering may take place in the following structures or materials:

1. **Shield around the source**
   -This phenomenon is used in the shield analysis
   -Scattering from the shield is the dominating factor for massive shields, > 1 cm Pb
   -The response is known to be linear [NKS-399]
2. **Source itself**
   -The source may be a macroscopic object and scattering can take place within the source itself
3. **Structural materials near the source**
   -Any surface near the source may cause scattering
4. **Ground surface between the source and the detector**
   -Scattering depends on the source-to-detector distance and the height of the source and the detector
5. **Air between the source and the detector**
   -The scattering depends mainly on source-to-detector distance
6. **Detector enclosure**
   -Some scattering takes place in the detector enclosure. This contribution should be constant for a given detector
7. **Coherent scattering**
   -Coherent scattering cross section is small but nevertheless important for the step (and also plays a role in peak ratio analysis)

Careful measurement campaigns and Monte Carlo simulations would help to clarify the scattering contribution of the items 1–7. These studies lead to understanding of the step height when there is no shielding material between the source and the detector.

2.2 Theory

As mentioned above, the concept behind the SR method is based on small angle scattering in e.g. a shielding material, and the step ratio is defined as

$$SR(E,x) = \frac{H(E,x)}{A(E,x)} \tag{2.2}$$

where *H*(*E,x*) is the height of the step (unit 1/keV), and *A*(*E,x*) is the peak area at energy *E* for the measurement when an attenuating material is present between a source and a detector. *H*(*E,x*) should be measured as close as possible to the peak of interest to minimize the bias due to interfering peaks, see Figure 2.1. High resolution of the detector system, like for the HPGe detector, is an advantage, especially if e.g. background peaks are significant.

SR(*E,x*) can be measured for different materials and thicknesses giving a calibration function which can be used in unknown situation for estimation of a shield thickness. Moreover, with the detector calibration and the shield thickness the source activity can be calculated. It is important though that the measurement set-up is similar to the calibration set-up, since Eq. 2.1 only is valid when the measurement is done under the same conditions as the calibration. If this is not true, the result will be a bias in the thickness measurement, see below.

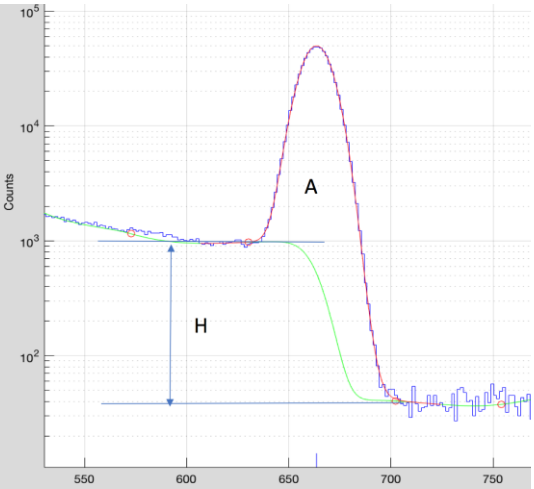

Figure 2.1 Definition of step height H(E,x) (1/keV). H(E,x) can also be understood as an area of a rectangle having a width of 1 keV.

2.3 Impact of the environment

It can be shown that when no other material than the shield is causing scattering, the *SR* as a function of shield thickness *x* can be written as (see Appendix 1)

$$SR = kx \tag{2.3}$$

This relationship was confirmed by Monte Carlo (MC) simulations, see Appendix 2. It was also shown *via* MC simulations that, in particular for low energy gamma photons, the surroundings like material close to the source as well as the ground might cause some small angle scattering resulting in an off-set in Eq. (2.3), see Appendix 2 and 3. This off-set was observed in the NKS project 2017, and will cause a bias in the shield analysis. The contribution from the ground can be reduced if the source and/or the detector is positioned at an elevated height. Normally, the height of the source will be fixed, but the height of the detector can be increased. For a source-to-detector distance of 10 m for a detector at a height of 1 m, the critical height, i.e. the height when no small angle scattering from ^{60}Co can contribute to the *SR*, is 10 cm, see Appendix 3.

Other contributions to the step origins from air between a source and a detector, the casing of a source, the source matrix, the detector endcap, and the dead layer of a p-type detector. Simulation of an extended source ^{137}Cs (d=3 mm, L=7 mm) 5 m from a detector with an aluminium endcap of 1 mm, air between the source and the detector, 3 mm of steel casing and 1 mm of dead layer resulted in a step ratio of about 0.00068. This step ratio would be equivalent to an iron thickness of about 3.9 mm based on the calibration shown in Figure 2.2.

2.4 Measurements

A ^{137}Cs source with a nominal activity of 1.8 GBq was measured. First, a calibration function was established using seven different thicknesses of iron, see Figure 2.2. Observe the deviation from zero in the function when *x*=0. A discussion on this can be found above and in Appendix 2 and 3. Thereafter a measurement was performed with a shield thickness of 5.5 cm. The thickness of the iron shielding in the measurement was measured to be (5.26±0.61) cm, *k*=2. The uncertainty here is a factor of about 1.6 higher compared to the 3.9 mm caused by a step ratio contribution from 1 mm of dead layer, 1 mm of aluminium detector casing, 3 mm of source steel casing, source matix and 5 m of air between the source and the detector.

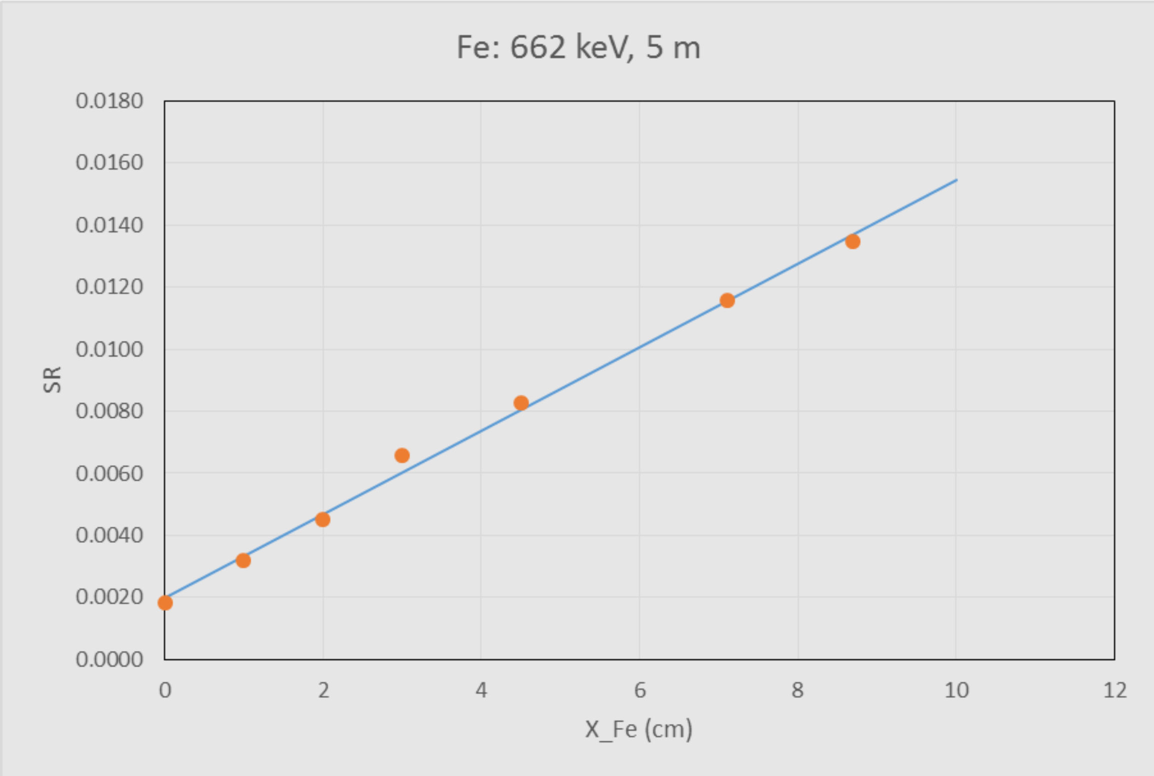

Figure 2.2 Calibration curve for the SR as a function of Fe thickness for E_γ=662 keV.

Knowing the source-to-detector distance and the efficiency of the detector the activity was estimated to (1.54±0.56) GBq, *k*=2, which should be compared to the nominal activity of 1.8 GBq. The probability density function for the thickness was relatively symmetric. However, due to the non-linearity introduced by the shielding factor *F*, see Eq. (3.3) below, the distribution of the activity might become skewed. In this case the 95.45% confidence interval (probabilistically symmetric) was [1.08, 2.23] GBq. Comparison to the (1.54±0.56) GBq from uncertainty propagation shows some non-symmetry of the probability density function.

3. Peak area ratio for shielding analysis

3.1 Calculation of shield thickness and source activity

If a radionuclide emits more than one gamma photon in its decay, the difference in the attenuation of two photons can be used to calculate the thickness of the shielding material. In the case the source radionuclide is a single photon emitter, like ^{137}Cs, the SR method has to be used. It should be pointed out though that the difference in energy between the two gamma photons should not be too small, since then the difference in attenuation will be small and the uncertainty of the thickness might become large. For an unshielded source the detector efficiency at a distance *r* and at the gamma energy *E* is

$$\varepsilon(r,E)=\left(\frac{r_0}{r}\right)^2 e^{-\mu_{air}(E)(r-r_0)}\varepsilon(r_0,E). \tag{3.1}$$

Here, $\varepsilon(r_0,E)$ is the efficiency at the gamma energy *E* at a reference distance r_0, and μ_{air} is the attenuation coefficient in air for a gamma photon with energy *E*. Ideally, *r* and r_0 should be large enough in order for the point source approximation to be valid. Moreover, the count rate C_A in a peak with energy E_A at a distance *r* is

$$C_A(r,E_A) = A_S\gamma_A\varepsilon(r,E_A)F(E_A) \tag{3.2}$$

where A_s is the activity of the source, γ_A the photon emission probability for the emitted photon having energy E_A, and $F(E_A)$ is the attenuation due to the shielding. For a Pb shield with thickness X_{Pb}, $F(E_A)$ can be expressed as

$$F(E_A)=e^{-\mu_{Pb}(E_A)X_{Pb}}. \tag{3.3}$$

If we now consider a second gamma photon with energy E_B emitted by the radionuclide in the source, we can calculate the net area ratio of the two peaks

$$\frac{C_A(r,E_A)}{C_B(r,E_B)} = \frac{\gamma_A}{\gamma_B}\frac{\varepsilon(r,E_A)}{\varepsilon(r,E_B)}e^{-[\mu_{Pb}(E_A)-\mu_{Pb}(E_B)]X_{Pb}} \tag{3.4}$$

In combination with Eq. 3.1 we get

$$\frac{C_A(r,E_A)}{C_B(r,E_B)} = \frac{\gamma_A}{\gamma_B}\frac{\varepsilon(r_0,E_A)}{\varepsilon(r_0,E_B)}e^{-[\mu_{air}(E_A)-\mu_{air}(E_B)](r-r_0)}e^{-[\mu(E_A)-\mu(E_B)]X_{Pb}}. \tag{3.5}$$

Rearranging Eq. 3.5 gives

$$\frac{C_A(r,E_A)\gamma_B\varepsilon(r_0,E_B)}{C_B(r,E_B)\gamma_A\varepsilon(r_0,E_A)} = e^{-[\mu_{air}(E_A)-\mu_{air}(E_B)](r-r_0)}e^{-[\mu(E_A)-\mu(E_B)]X_{Pb}} \tag{3.6}$$

Ignoring the attenuation in air, which was done in this work, simplifies this equation to

$$\frac{C_A(r,E_A)\gamma_B\varepsilon(r_0,E_B)}{C_B(r,E_B)\gamma_A\varepsilon(r_0,E_A)} = e^{-[\mu(E_A)-\mu(E_B)]X_{Pb}} \tag{3.7}$$

Taking the logarithm of Eq. 3.7 gives

$$X_{Pb} \approx -\frac{\ln(K)}{\mu_{Pb}(E_A)-\mu_{Pb}(E_B)} \tag{3.8}$$

where

$$K = \frac{C_A(r,E_A)}{C_B(r,E_B)}\frac{\gamma_B}{\gamma_A}\frac{\varepsilon(r_0,E_B)}{\varepsilon(r_0,E_A)} \tag{3.9}$$

With the measured shield thickness X_i, the shielding factor e.g. $F(E_A)$ can be calculated using Eq. 3.3, and finally the source activity using Eq. 3.2 after solving for A_s.

For situations where the difference in the distance for the measurement and the reference distance r_0 is short, $r-r_0<10$ m, the difference in shield thickness is less than 0.7 mm for the two peaks of ^{60}Co if the attenuation in air is ignored. However, for very long distances relative to the reference distance, Eq. 3.6 should be used for calculation of shield thickness. Observe that for a shield thickness measurement only the relative efficiencies are needed and not the absolute ones. However, absolute efficiencies would of course be needed for activity calculations.

The method is sensitive to uncertainties in the number of counts of the two gamma peaks, the uncertainty in mass attenuation coefficients and the uncertainty in the efficiencies. Normally the uncertainty in a photon emission probability is low enough in order to not contribute to the combined uncertainty of either the shield thickness or the source activity. For a thickness measurement the ratio of the efficiencies used, and the uncertainty of this ratio might likely be significantly lower than the uncertainties of the efficiencies due to correlations. Furthermore, the uncertainty in the mass attenuation coefficients is around 1-2%. However, this uncertainty is probably due to uncertainties from the function fit of measured data. Therefore, they are correlated, and if the difference in gamma energies are small the uncertainties of two mass attenuation coefficients will mostly cancel out in the calculation of the difference.

3.2 μ_{tot} vs. (μ_{tot}-μ_{coh})

In the project in 2017 it was observed that the use of total attenuation coefficients resulted in erroneous results for hand calculations since the measurement set-up was not for a narrow beam. Subtracting the coherent scattering from the total attenuation gave correct results. A justification for this is shown in Appendix 2 and 4.

3.3 Shield thickness and source activity calculations

Measurements of shield thicknesses and source activities were done for ^{60}Co with lead shielding, ^{152}Eu with iron shielding and ^{131}I with iron shielding. The results of these measurements are summarised in Table 1.

Table 1 Measurements of shield thicknesses and source activities. The uncertainties u_{Xmeas}, and u_{Ameas} were calculated using uncertainty propagation in accordance with GUM [GUM1]. Confidence intervals, CI, were calculated using propagation of distributions using Monte Carlo calculations [GUM2]. In the latter case, CI represents a probabilistic symmetric interval of 95.45%.

Radionuclide	Nominal Activity	Shield	X_{meas}, k=2	95.45% CI from MC	A_{meas}, k=2	95.45% CI from MC
^{131}I	80±8 MBq	1 cm Fe	(1.17±0.30) cm	0.87-1.48 cm	(78±17) MBq	63-98 MBq
^{131}I	80±8 MBq	4.7 cm Fe	(4.85±0.34) cm	4.50-5.20 cm	(74±19) MBq	57-95 MBq
^{152}Eu	585±90 MBq	1 cm Fe	(0.63±0.52) cm	0.12-1.16 cm	(490±120) MBq	390-630 MBq
^{152}Eu	585±90 MBq	5.5 cm Fe	(5.5±1.1) cm	4.4-6.7 cm	(530±260) MBq	330-870 MBq
^{60}Co	4.3 GBq	1 cm Pb	(0.87±0.74) cm	0.14-1.6 cm	(3.9±2.0) GBq	2.4-6.4 GBq
^{60}Co	4.3 GBq	5 cm Pb	(4.90±0.88) cm	4.0-5.8 cm	(3.7±2.2) GBq	2.1-6.7 GBq
^{60}Co	4.3 GBq	10 cm Pb	(9.3±2.2) cm	7.2-12 cm	(2.8±4.0) GBq	0.70-12 GBq

The activities of the sources at the time of measurement were (80±8) MBq for ^{131}I, (585±90) MBq for ^{152}Eu and 4.3 GBq (uncertainty unknown) for ^{60}Co. From Table 1 it can be concluded that all measurements, shielding thickness and activities, were consistent with the known values.

The confidence intervals, CI, of the shielding thickness measurements are relatively symmetric. However, when the uncertainty from the shielding measurement becomes large in combination with large attenuation, the shielding factor F (Eq. 3.3) will be skewed due to non-linearity introduced by the exponential function in Eq. 3.3. In such cases uncertainty propagation will give erroneous results for the CI of the activity, e.g. resulting in a probability distribution function of the activity including negative values. Therefore, Monte Carlo calculations of the uncertainties were done as well on all these measurements. Figure 3.1 shows the probability density function for a ^{60}Co source shielded with 10 cm of lead. Observe that the probability that the evaluated activity is less than zero when uncertainty propagation is used.

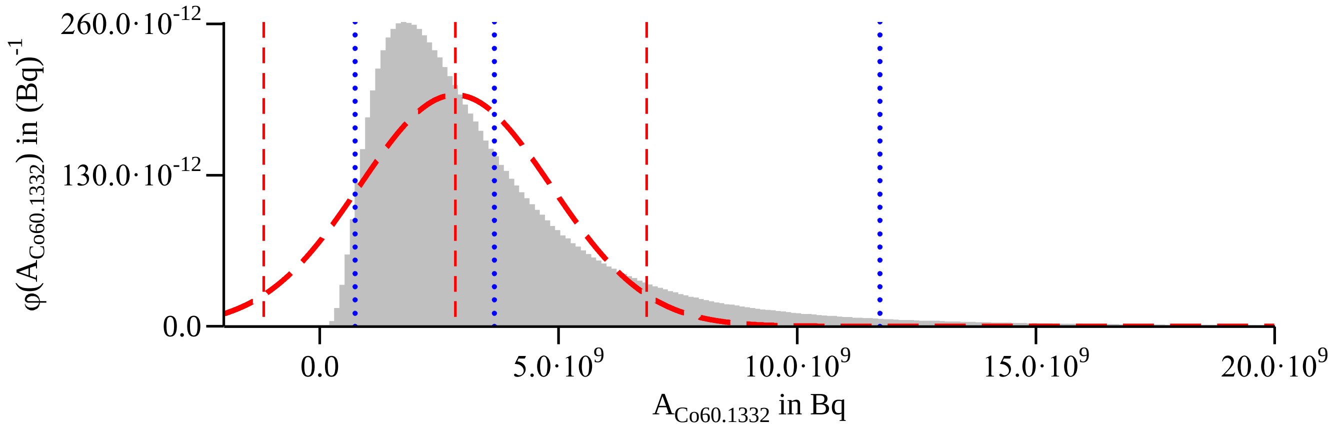

Figure 3.1 ***Probability density function for a measurement result of a ^{60}Co source shielded with 10 cm of lead. Blue vertical lines define the 95.45% confidence interval and the mean value from the Monte Carlo calculation; Red vertical lines is the 95% confidence interval based on uncertainty propagation and its mean value; Red dashed curve is the probability density function based on uncertainty propagation.***

4. Source localization

Localization of a radioactive source is essential in order to find and recover the source. Localization can be achieved using triangulation, i.e. perform at least two measurements at different directions to a source. In this study an instrument (RanidSOLO, Environics, Finland) was used. The localization principle of the instrument is anti-collimation, utilizing a rotating attenuator causing a dip in the instrument response in the direction of the source when the attenuator is positioned between the detector and the source. Based on the directions of the two measurements and the distance between them, the location and the distance from the measurement positions can be estimated, see Appendix 5. The results showed that with the instrument used, the direction can be estimated within 7-10 degrees, and the distance within 10-25%.

Another possibility for source localization is the use of cps values of a peak at three locations. This idea was tested in the measurement campaign. The results were promising and showed that the method works for an unshielded source (^{137}Cs), see Appendix 6. However, photon attenuation in the air and in the shield, when it is different to different directions, complicates the analysis.

5. Conclusions

Activity measurements of shielded sources were studied in this work, including the contribution of source shielding. The work shows that activities of shielded sources can be measured with uncertainties that would be fit-for-purpose in e.g. a nuclear security event. Moreover, a thorough investigation of factors influencing the uncertainty of the activity measurements was done. It showed that for example the detector height above the ground and the height of the source itself are important factors contributing to the step of a peak which is used to estimate the shield thickness. By increasing the height of the detector, this confounding contribution can be decreased.

Measurements of source position was also done, which showed that direction to a source could be estimated within 7-10 degrees, and the distance within 10-25%.

The main outcome of this project is that in a nuclear security event, or in other emergencies, involving shielded radioactive sources, threat assessment becomes more reliable since the activity of shielded sources can be measured with an uncertainty that would be-fit-for purpose.

6. References

GUM1 JCGM 100:2008, 2008. GUM 1995 with minor corrections. Evaluation of measurement data—Guide to the expression of uncertainty in measurement.

GUM2 JCGM 101:2008, 2008. Evaluation of Measurement Data-Supplement 1 to the “Guide to the Expression of Uncertainty in Measurement”-Propagation of Distributions Using Monte Carlo Methods.

NKS-399 H. Toivonen, M. Granström, G. Ågren, G. Jónsson, B. Møller, P. Roos, H. Ramebäck, *Activity estimation of shielded or hidden radionuclides in emergency conditions*, NKS-399, December 2017

Appendix 1 Justification for the linear response of the step ratio

NKS RadShield2 measurement campaign

Umeå, 22-23 Aug 2018

Sakari Ihantola, Radis Technologies

Harri Toivonen, HT Nuclear

Let us consider a beam of photons with energy *E* approaching a shield. The main beam is attenuated exponentially as a function of distance traversed and simultaneously some photons scatter to different angles (Compton scattering). We are interested in those photons that have energy between (*E* , *E'*) where *E'* = *E* - ΔE); ΔE ≅ 10 keV. These photons produce a step in the spectrum just below the photopeak.

The step ratio after the beam has traversed a distance of *x* is

$$SR = \frac{H(x)}{A(x)} \qquad (1)$$

where *A(x)* refers to the primary peak area and *H(x) to* the step area (1/keV). *SR* is also the ratio of the beam intensities because the full-energy absorption probability (efficiency of the detector) is almost the same for photons with Energy *E* and *E'*. Therefore

$$SR = \frac{I_s(x)}{I_p(x)}. \qquad (2)$$

where $I_p(x)$ and $I_s(x)$ are the beam intensities for the primary beam and the scattered radiation. They will be attenuated in the medium with coefficients μ_p and μ_s. Obviously

$$I_p(x) = I_0 e^{-\mu_p x} \qquad (3)$$

and

$$\frac{dI_s(x)}{dx} = -\mu_s I_s(x) + kI_p(x). \qquad (4)$$

The first part on the right side of Equation (4) describes the attenuation of the scattered photons and the second part their production, *k* being the scatter probability. The solution is straightforward and gives

$$SR = \frac{I_s(x)}{I_p(x)} = \frac{kI_0}{\mu_s - \mu_p} \frac{\left[e^{-\mu_p x} - e^{-\mu_s x}\right]}{I_0 e^{-\mu_p x}} = \frac{k}{\mu_s - \mu_p}\left[1 - e^{-(\mu_s - \mu_p)x}\right]. \quad (5)$$

Because $\mu_s \cong \mu_p$, then

$$SR = kx. \quad (6)$$

Appendix 2 Monte Carlo simulations of step ratio and peak area ratio with Geant4

NKS RadShield2 measurement campaign

Umeå, 22-23 Aug 2018

Sakari Ihantola, Radis Technologies

Abstract

Key results of the Monte Carlo simulation studies are presented. The simulations confirmed that the step ratio caused by a shielding material between the detector and the source depends linearly on the shield thickness. Some step can also be caused by other structures that are not on the line-of-sight between the source and the detector. However, the step caused by these other structures is typically so small that it can be ignored in the estimation of the activity of an unknown shielded source. If the shielding thickness and source activity are estimated based on the ratio of two peaks, the attenuation in the shielding can be calculated by hand. The attenuation coefficient used in the hand calculations should be the total attenuation coefficient without coherent scattering.

Software code

Simulations were performed with Geant4 software code version 10.04.p02. The standard physics list used in the simulations included G4DecayPhysics, G4RadioactiveDecayPhysics and G4EmStandardPhysics.

The simulated gamma ray energies were 59.5, 364.5, 637.0, 661.7, 1173.2 and 1332.5 keV. The gamma rays were emitted uniformly within a 45-degree angle towards the detector. The limited emission angle was taken into account in the data analysis.

Geometry

The simulation geometry consisted of Ortec Detective germanium crystal at 1.0 m distance from the source. The distance is measured from the detector end cap. The detector enclosure was not included in the simulations, but the detector dead layer was. The simulation volume (world) was filled with air.

Step caused by a shield

The purpose of this study was to investigate:

a) The dependency of the step ratio on the shield thickness. The hypothesis is that the step ratio depends linearly on the shield thickness.
b) The magnitude of the step caused by the shield. This is important for evaluating the significance of the step caused by other structures (see Section 4).

The simulation geometry is shown in Figure 1.

The simulation results are presented in Figures 2 and 3. As can be seen, the hypothesis was correct and the step ratio depends linearly on the shield thickness. The step ratio is largest for low-energy gamma rays measured through a thick shield.

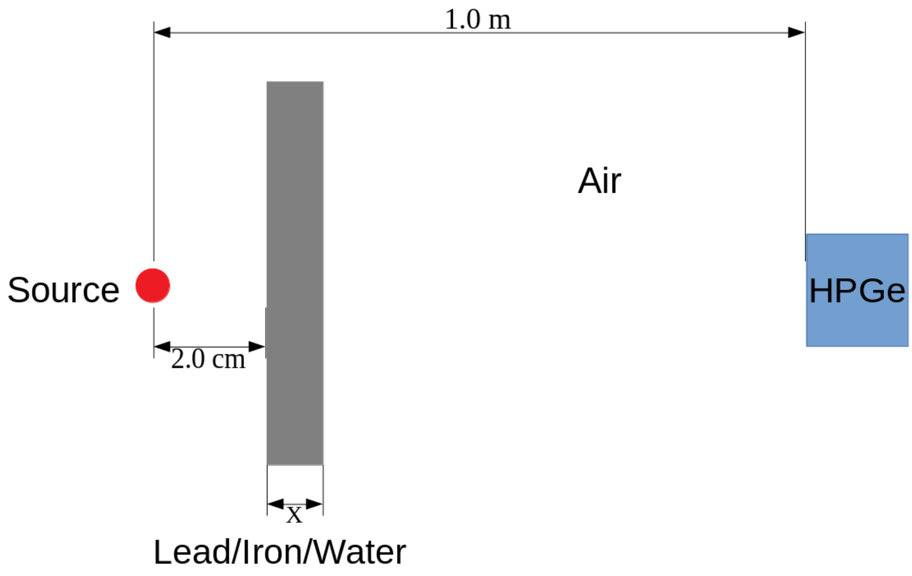

Figure 1. Simulation geometry used to study the step ratio caused by the shield.

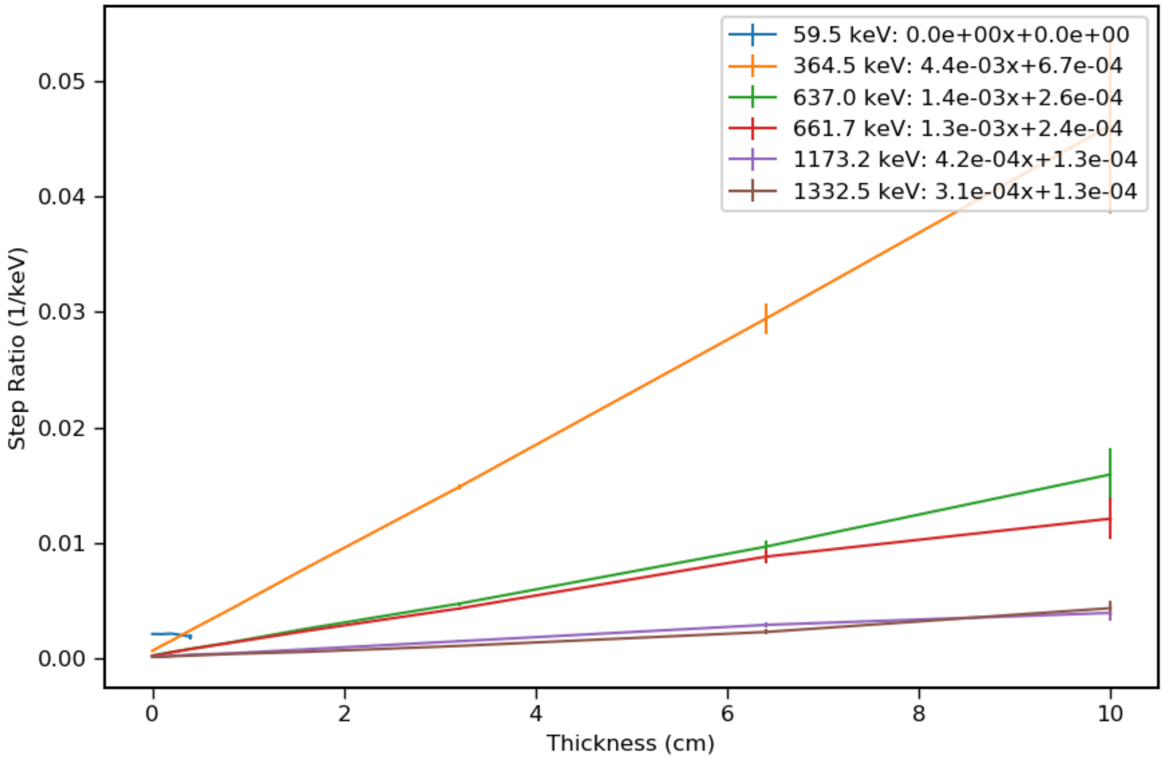

Figure 2. ***Step ratio as a function of the thickness of the iron shield. According to the plot, the step ratio depends linearly on the shield thickness. Due to the ideal simulation geometry that does not include the detector enclosure or other surrounding materials, the step ratio is almost zero without the shield (shield thickness zero).***

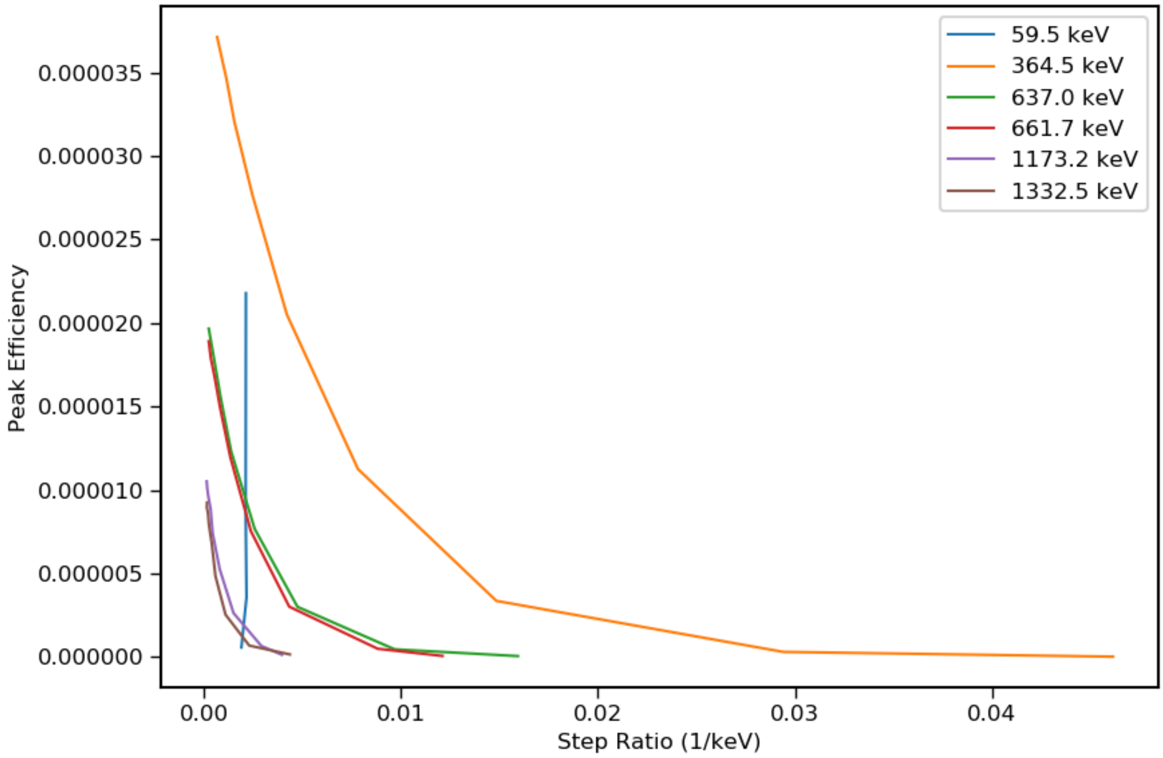

Figure 3. ***Peak efficiency through an iron shield as a function of the step ratio. The thickness of the iron shield was varied from 0 to 10 cm. The distance from the source to the detector end cap was 1.0 m.***

Step caused by other structures

The purpose of this study was to investigate:

a) How large a step ratio can be caused by structures other than the shield.
b) The error in activity calculation, if the step caused by these other structures is misinterpreted as caused by the shield.

The structures studied are ground and a small slab of material next to the source. The simulations geometries are presented in Figures 4 and 5.

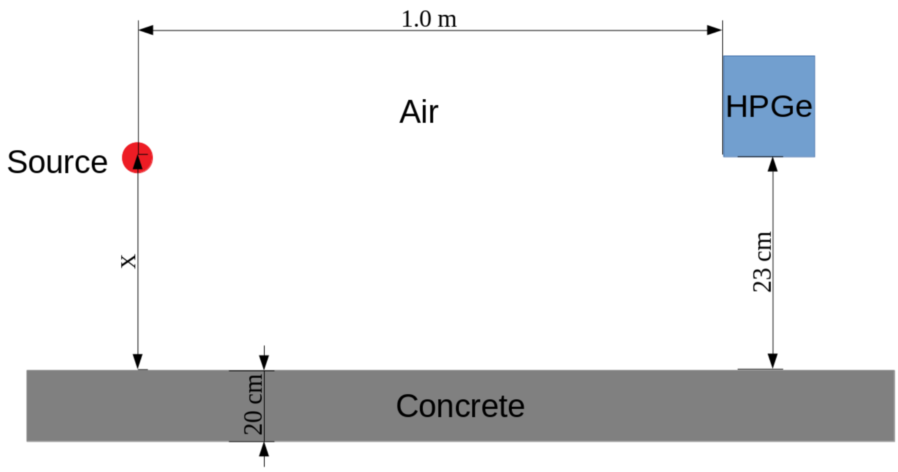

Figure 4. ***Simulation geometry used to study the step ratio caused by the ground. The detector height above the concrete floor was fixed at 230 mm (measured to the closest point of the crystal surface) and the source height was varied. The distance from the source to the detector end cap was 1.0 m. The detector height was selected such that if all dimensions are multiplied by five, the geometry is close to the one used during the measurements at FOI.***

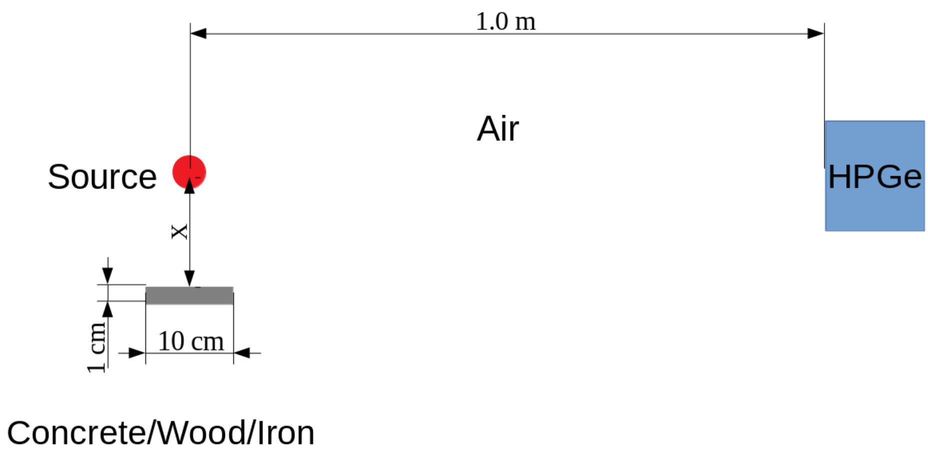

Figure 5. ***Simulation geometry used to study the step ratio caused by a 10 cm x 10 cm x 1 cm slab of material near the source.***

The simulation results are presented in Figures 6 and 7. As can be seen, both the floor and the small slab can cause a noticeable step in the spectrum if the source energy is low. However, a similar step is also caused by an iron shield with a thickness of less than 1.0 mm. Therefore, the influence of the ground and other materials near the source can typically be ignored when the activity of an unknown shielded source is estimated based on the peak ratio.

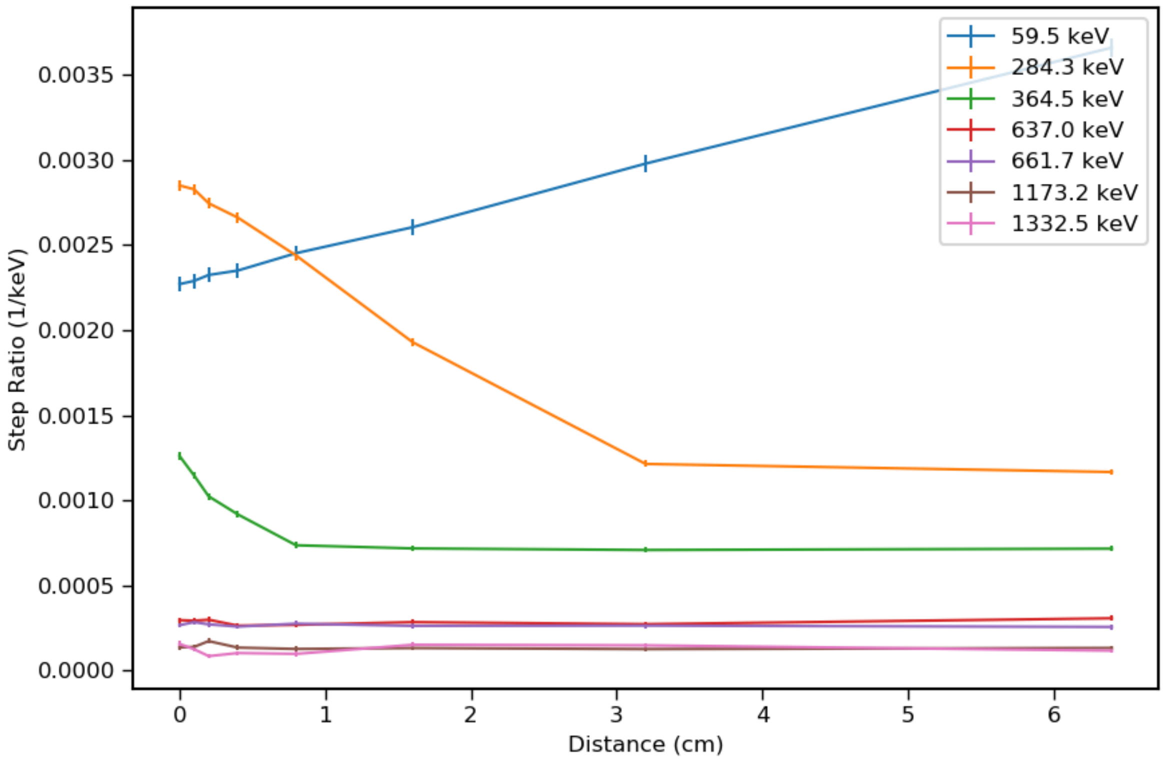

Figure 6. Step ratio as a function of the distance of the source to the concrete floor. As can be seen, a floor close to the source can cause a noticeable step in the spectrum if the source energy is low.

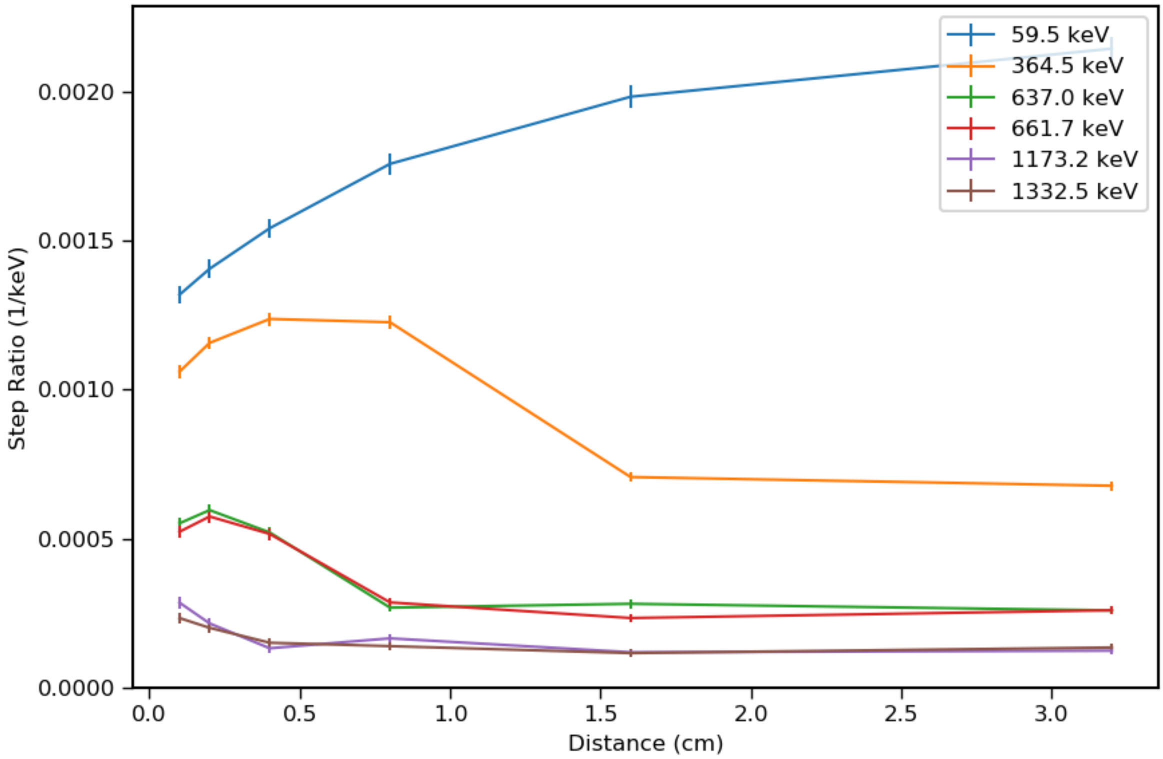

Figure 7. ***Step ratio as a function of the source distance from a 10.0 x 10.0 x 1.0 cm3 slab of iron. As can be seen, the structures around the source can cause a noticeable step in the recorded spectrum.***

Coherent scattering

The purpose of this study was to investigate if the attenuation caused by the shield can be calculated by hand without using Monte Carlo simulations. The hypothesis is that the calculation by hand gives the correct outcome if the coherent scattering is subtracted from the total attenuation coefficient used in the calculation. This is based on the assumption that for coherent scatter from the shield, the probability of scatter in and scatter out are equal.

The simulations geometry is presented in Figure 8.

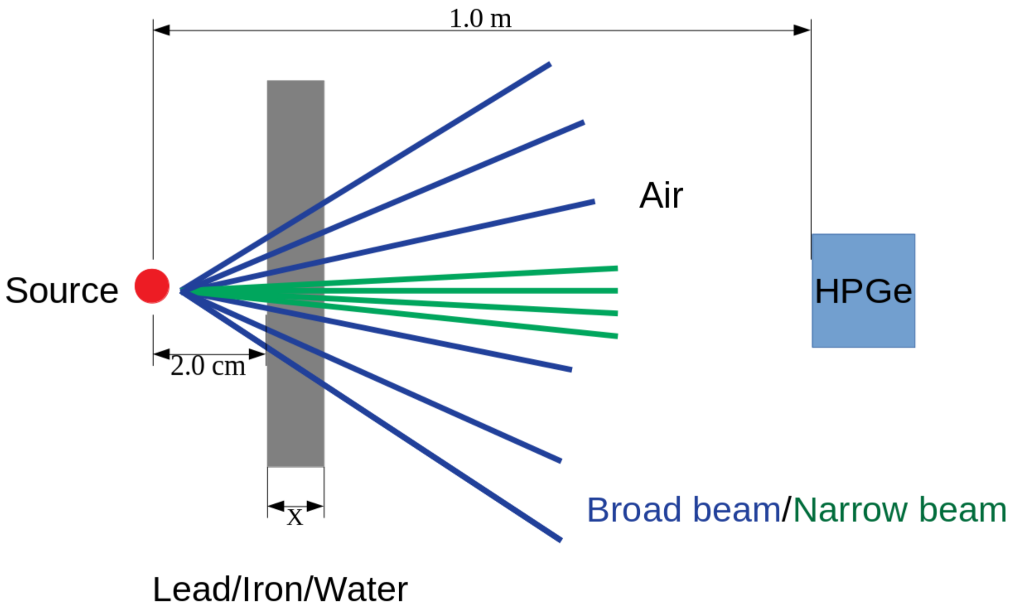

Figure 8. ***Simulation geometry used to study the effect of coherent scattering on peak efficiency. The simulations were repeated with narrow (2.0 deg) and and broad (45.0 deg) beam geometry both with coherent scattering activated and inactivated.***

The simulation results are presented in Figures 9, 10 and 11. The results support the hypothesis that the narrow beam simulations (analogous to calculations by hand) give the correct outcome if the coherent scattering is not considered. However, the influence of coherent scattering on step ratio is often small and can be omitted on practical analysis.

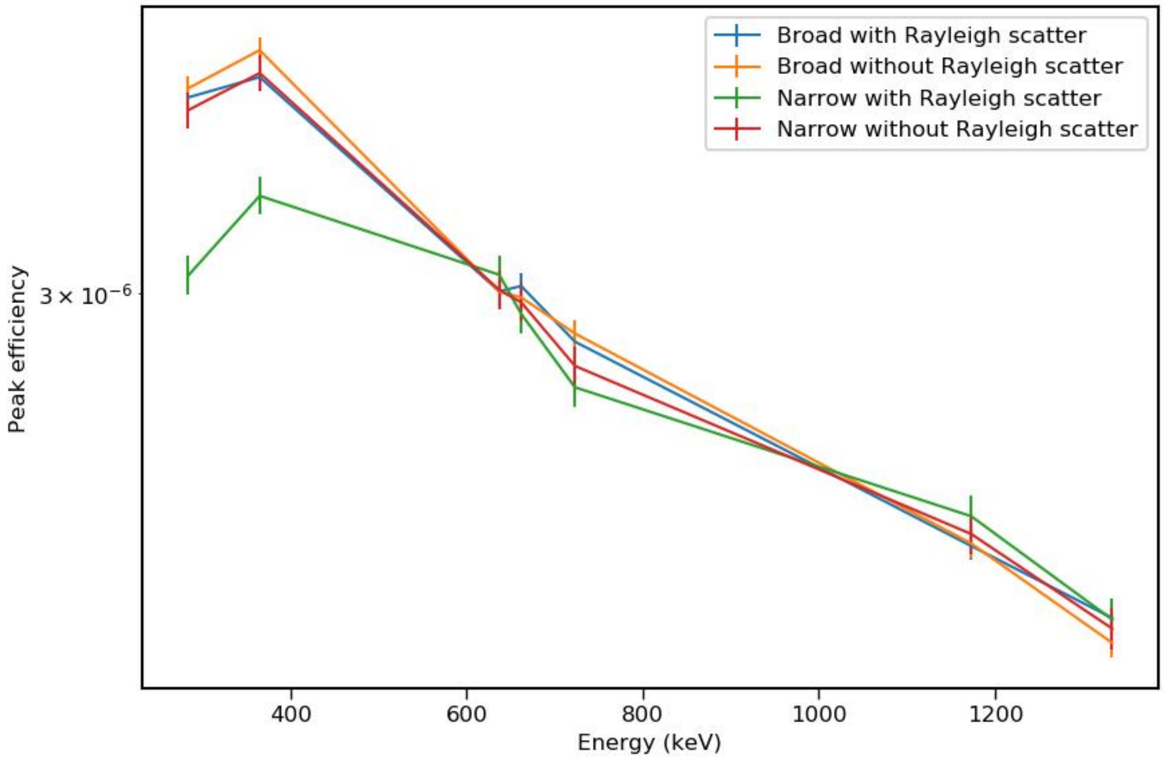

Figure 9. Peak efficiency through a 32.0 mm iron shield. The simulation was repeated both in narrow (2 deg) and broad (45 deg) beam geometry with coherent scatter activated and inactivated. Only the narrow beam simulation with coherent scatter activated differs significantly from the other simulation results.

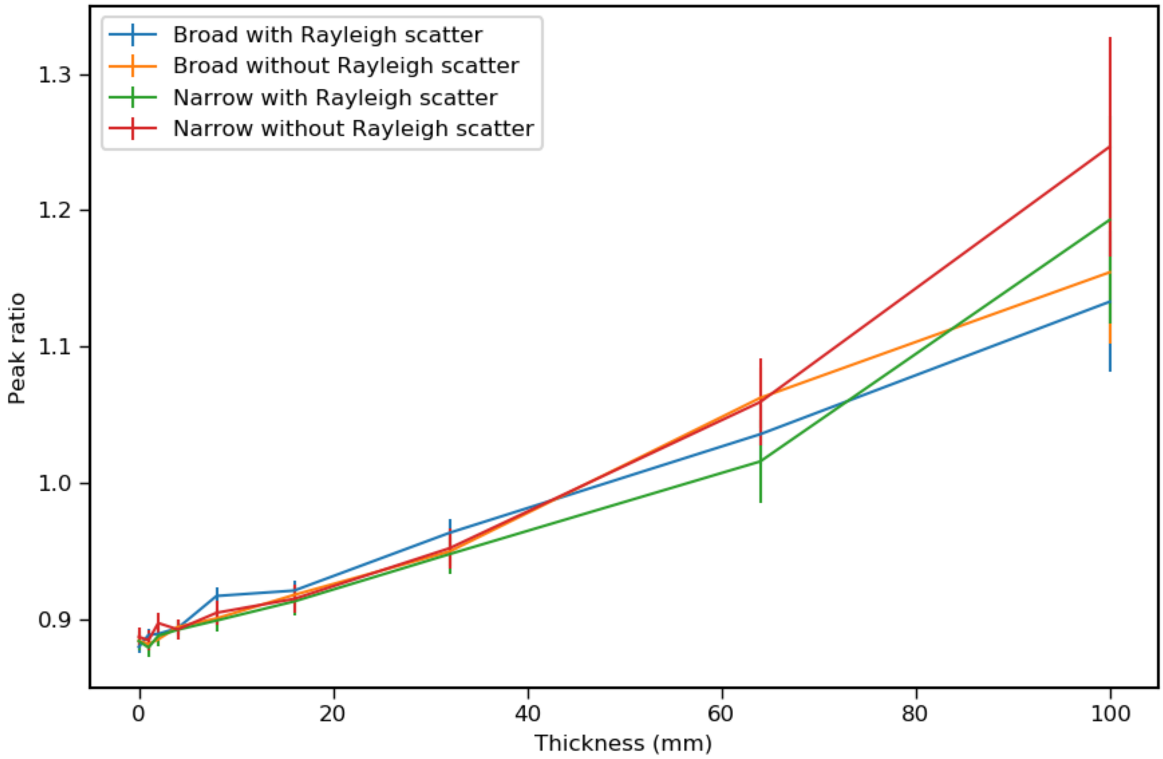

Figure 10. ***^{60}Co (1332.5 keV / 1173.2 keV) peak area ratio as a function of the thickness of an iron shield. The simulation was repeated both in narrow (2 deg) and broad (45 deg) beam geometry with coherent scatter activated and inactivated. The simulation results do not differ significantly from each other.***

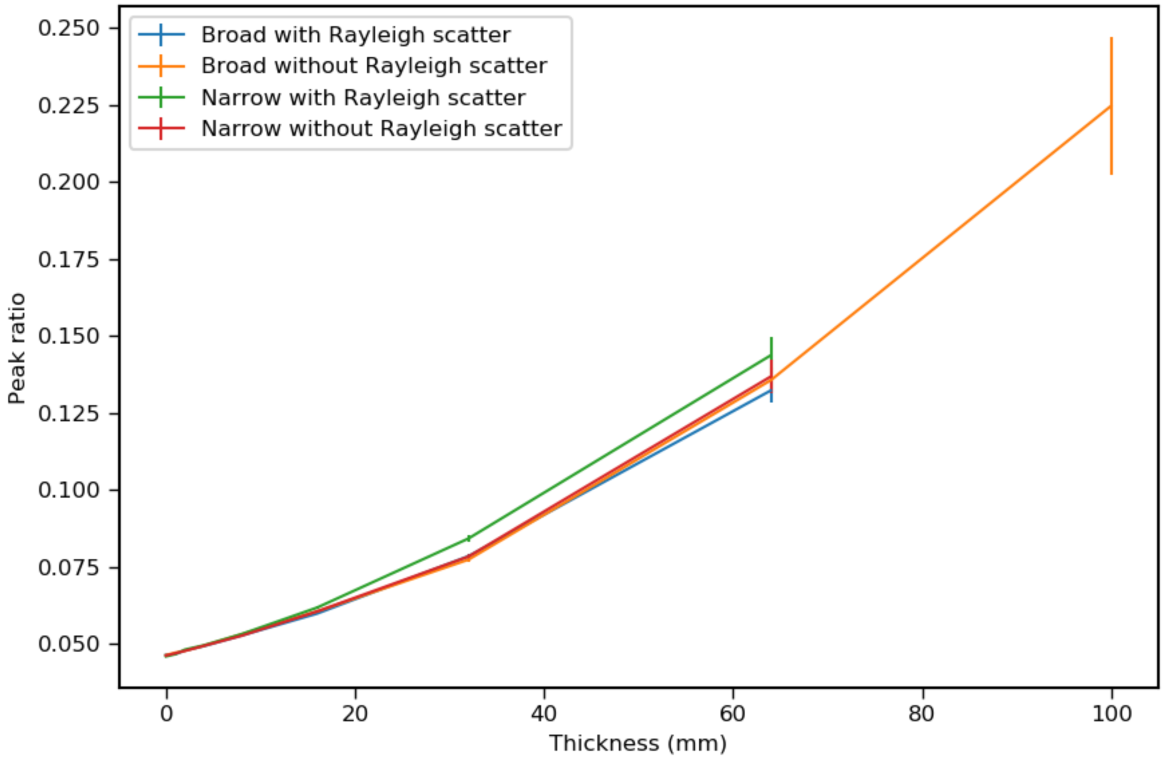

Figure 11. ***[131]I (637.0 keV / 364.5 keV) peak area ratio as a function of the thickness of an iron shield. The simulation was repeated both in narrow (2 deg) and broad (45 deg) beam geometry with coherent scatter activated and inactivated. Only the narrow beam simulation with coherent scatter activated differs significantly from the other simulation results.***

Appendix 3 Impact of environment to step ratio in shield thickness analysis

NKS RadShield2 measurement campaign

Umeå, 22-23 Aug 2018

Harri Toivonen, HT Nuclear

Mikko Kilkki, Environics

Sakari Ihantola, Radis Technologies

Abstract

The step ratio is a property of the shield around the source. The response is a linear function of thickness. However, the step ratio is not zero when there is no shield. Environmental factors may play an important role. The impact of scattering from ground was studied experimentally. It was shown that the scattered photons do not cause a step on the low-energy side of the peak if the detector is placed above a certain critical height. This critical height depends on the overall measurement geometry. In operational measurements, the disturbance by surface scattering is minimized by placing the detector as high as possible above the ground (> 1 m).

Introduction

The NKS project 2017 showed that the slope of the response curve for the step ratio (*SR*) is a property of the shield, and it is linear in the parameter domain of interest (NKS-399). However, at thickness zero (no shield) *SR* seems to depend on environmental conditions. See parameter *C* = *SR*(0) in Figure 1. The following items may contribute to *C*: source itself (macroscopic object); structural materials near the source; ground between the source and the detector; air between the source and the detector; detector enclosure; coherent scattering.

The following analysis is aimed to confirm experimentally that indeed the environmental conditions play a role in step ratio analysis. The studies are focused on estimating the impact of the floor as a scattering surface to the step ratio, i.e., *SR*(0).

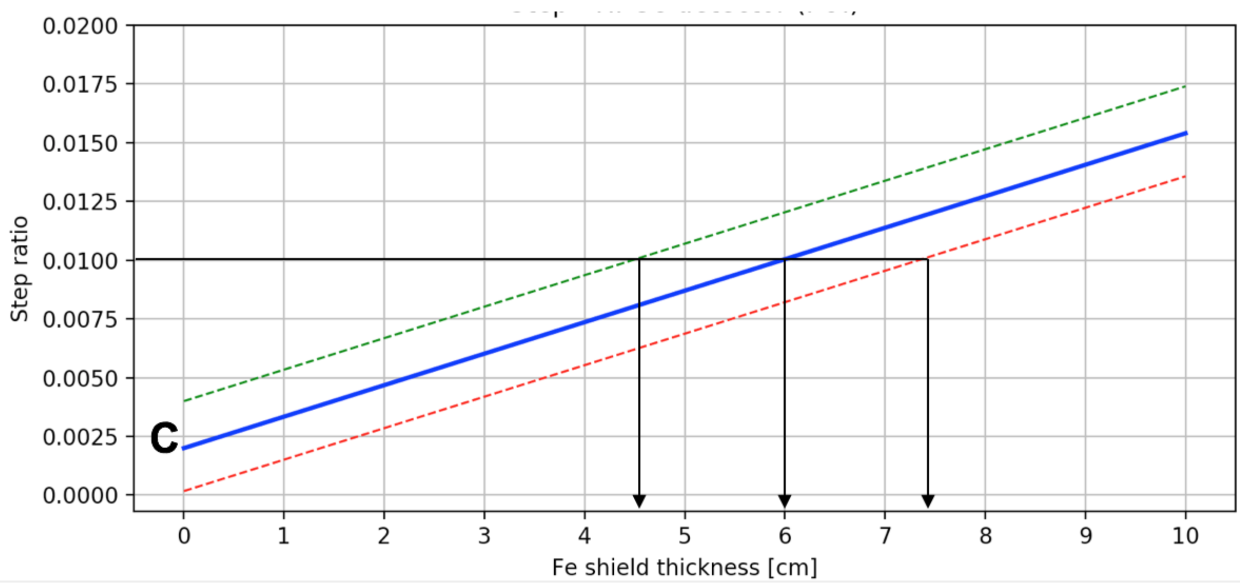

Figure 1. ***Step ratio in iron. The blue curve is measured by FOI in the NKS measurement campaign 2017 (HPGe detector and a ^{137}Cs source). The red curve is simulated (Sakari Ihantola, also 2017) assuming no scattering from the environment, except air. The green curve is hypothetical response in a challenging environment, say at long distances. As we see, considerable uncertainty is involved in the shield thickness analysis using the inversion of the calibration curves: Blue = 6.0 cm, Red = 7.4 cm, Green = 4.5 cm.***

Scattering from a surface - geometrical considerations in two dimensions

Let us define a critical angle θ above which the scattered photons cannot reach the detector in a measurement system; this means that they have lost more energy than ΔE (10 keV) from their original energy. For the geometry in two dimensions, see Figure 2.

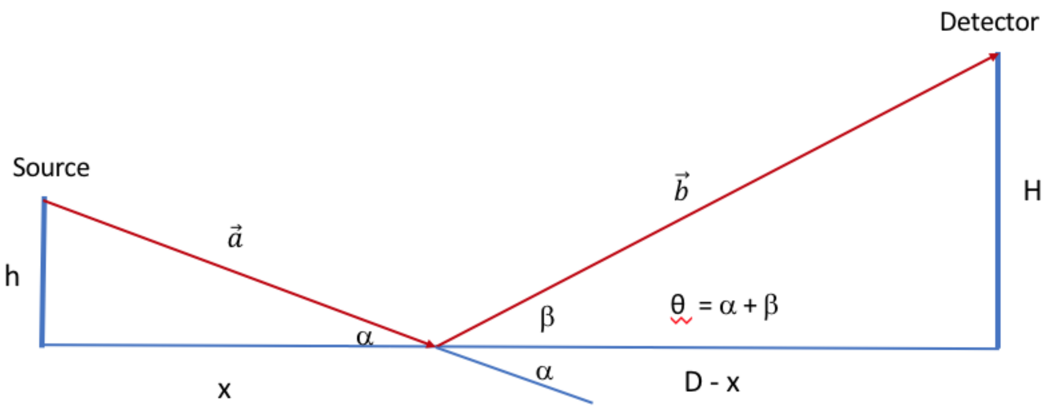

Figure 2. Compton scattering from a surface (line).

The geometry in Figure 2 defines an interval x ∈ (x_1, x_2) where the small-angle scattering is possible:

$$tan(\theta) = tan(\alpha + \beta) = \frac{tan(\alpha)+tan(\beta)}{1-tan(\alpha)tan(\beta)}\,. \quad (1)$$

Consequently,

$$tan(\theta) = \frac{\frac{h}{x}+\frac{H}{D-x}}{1-\frac{hH}{x(D-x)}} \quad (2)$$

which leads to a second order polynomial with solutions x_1 and x_2:

$$tan(\theta)x^2 + [(H-h) - tan(\theta)D]x + [D + tan(\theta)H]h = 0 \quad (3)$$

A more general approach to the scatter problem is based on vector calculations. Let us confirm the approach above by an alternative formulation:

$$cos(\theta) = \frac{\vec{a}\cdot\vec{b}}{\|\vec{a}\|\|\vec{b}\|}\,. \quad (4)$$

The dot product in two dimensions is

$$\vec{a}\cdot\vec{b} = x(D-x) - hH \quad (5)$$

and the norms

$$\|\vec{a}\| = \sqrt{x^2 + h^2} \quad (6)$$

$$\|\vec{b}\| = \sqrt{(D-x)^2 + H^2}\,. \quad (7)$$

Combining Equations (4) – (7) and performing some algebra gives Equation (3), as expected.

Vectors in 3D

Scattering takes place from ground surfaces. It is not limited to a line between the source and the detector. This means that the problem is truly three dimensional. Therefore let us define the coordinate system as follows: the scattering surface is in the (x,y) plane whereas the source and the detector are points above this plane (z coordinate).

A geometrical solution may be possible, but it seems to lead to complex equations. However, the vector calculus, based on Equation (5), is straightforward, and the result can be easily solved numerically (see Figure 3).

Small angle scattering takes place on a surface near the line between the source and the detector. Particularly at large distances, the environmental impact of scattering to the peak step may increase significantly. Therefore, the detector should be placed as high as possible above the ground level.

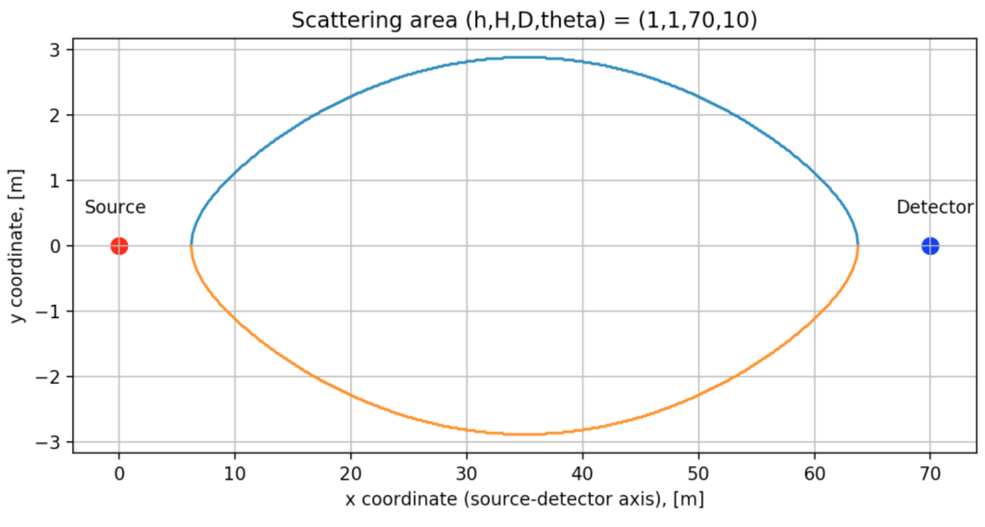

Figure 3. Scattering from ground surface when the source and the detector are at a height of 1 m and are separated 70 m from each other. The photons considered are scattered to angels smaller than 10 degrees. Note that x and y axes are not in the same scale (y axis blown up by 10).

Critical height of the source

In practise, the height of the source is fixed. Then it is useful to know the critical height of the source above which no small-angle scattering is possible from the surface to the detector. This is easy to calculate from Equation (4) by setting the discriminant of the quadratic equation to zero. Figure 4 gives a view to the solution of the problem. For example, when the source-detector distance is 10 m, no scattering with angles below 10 degrees takes place towards a detector at a height of 1 m from a source that is more than 10 cm above the ground level.

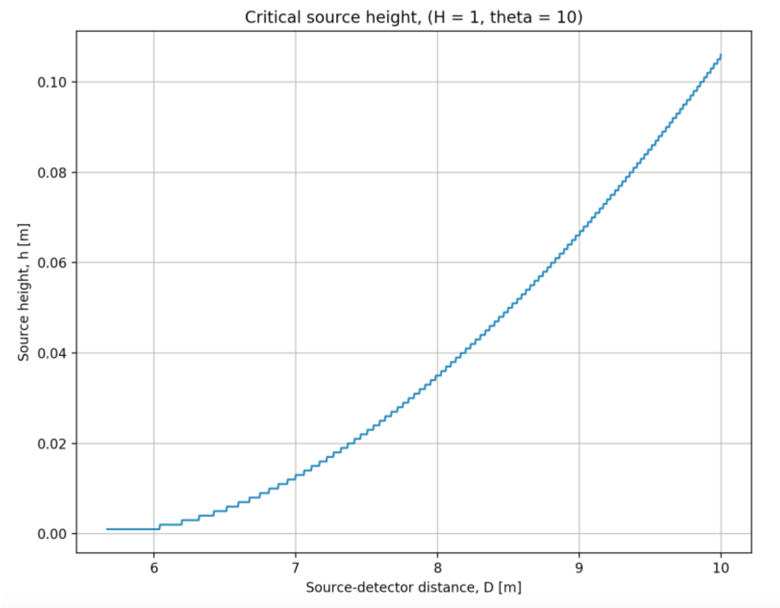

Figure 4. ***Critical source height for no scattering to detector from ^{60}Co. Scattering angle below 10 degrees and detector height 1 m.***

Scattering from a surface – $LaBr_3$ measurements with ^{137}Cs and ^{60}Co

Experiments were designed to test the theoretical considerations of the impact of scattering from a surface to the step ratio (Figure 5 and 6). The measurements were carried out in the FOI tent (10 x 15 m^2). The following source-detector distances (SDD) were chosen: 5 m for ^{137}Cs and 10 m for ^{60}Co.

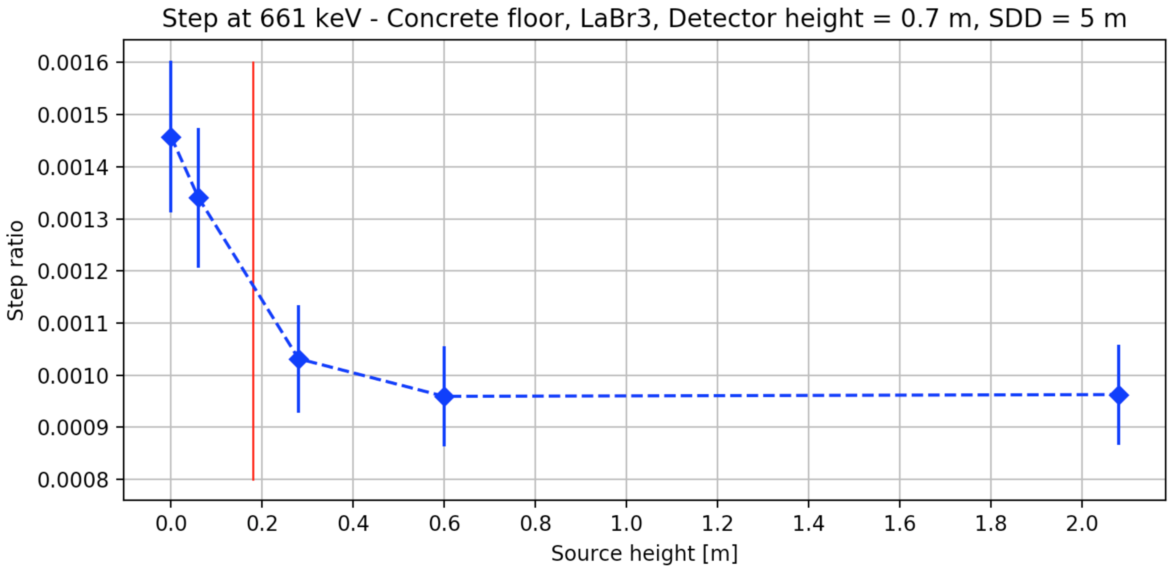

Figure 5. ***Step ratio as a function of source height above concrete floor for ^{137}Cs. The critical height for no scattering towards the detector is 0.18 m based on a separate analysis of scattering angles (15-18 degrees). The step analysis refers to the use of counts between 620-630 keV. In $LaBr_3$, energies 20 keV below the photo peak are masked by the peak itself and cannot be used for step analysis.***

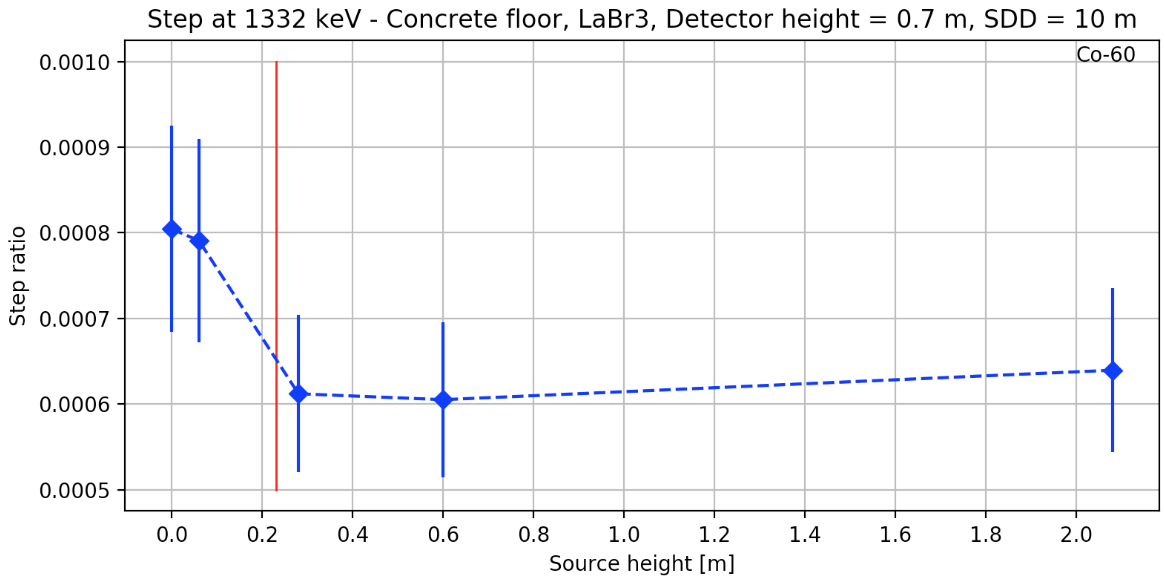

Figure 6. ***Step ratio as a function of source height above concrete floor for ^{60}Co. The critical height for no scattering towards the detector is 0.23 m based on a separate analysis of small scattering angles (about 10 degrees). The step analysis refers to the use of counts between 1275-1285 keV. In $LaBr_3$, energies 50 keV below the photo peak are masked by the peak itself and cannot be used for step analysis.***

Appendix 4 Peak area ratio in shield thickness analysis

NKS RadShield2 measurement campaign

Umeå, 22-23 Aug 2018

Harri Toivonen, HT Nuclear

Mikko Kilkki, Environics

Sakari Ihantola, Radis Technologies

Abstract

Peak area ratios were measured at energies 637, 364 and 284 keV of ^{131}I for a source-detector distance of 1 m. The counting geometry was varied by shielding the source with pieces of iron. The measurements revealed that subtracting the coherent scattering component from the total attenuation coefficient gives good nuclear data for the peak area ratio calculations. The predicted response is consistent with the measurements.

Introduction

The NKS Radshield project 2017 showed that the peak area ratio method works well for the shield analysis of emitters with multiple lines. Monte Carlo calculations explained nicely the peak area ratio as a function of the shield thickness. The experiments in 2017 were performed with a ^{60}Co source behind lead, iron, water and concrete shields. The exposure condition was not "narrow beam" and therefore the use of total attenuation coefficients gave wrong results in hand calculations. It turned out that subtracting the coherent scattering component (μ_{coh}) from the total attenuation coefficient (μ_{tot}) gives excellent prediction for the peak area ratio.

In 2017 no measurements were performed with low-energy emitters. The NKS measurement campaign, Radshield2, in 2018 included studies for the analysis of the peak area ratio at a wider range of energies than those of ^{60}Co emission lines (1173 keV and 1332 keV). The problem was approached in two ways: simulations (see appendix 2) and measurements with ^{131}I which has several emission lines of interest (see Figure 1). The measurements were deigned to verify the hypothesis of validity of the attenuation coefficients (μ_{tot} - μ_{coh}) in the shield analysis.

Measurements

In the present study, the peak area ratios were measured at energies 637, 364 and 284 keV. Other peaks were not considered because of their low emission yields and consequently poor statistics in counting. Several pieces of iron were used for the shielding. The thickness of the Fe plates varied between 0 – 4.7 cm. The measurements were performed at a source-detector distance of 100 cm using a $LaBr_3$ detector (1.5”x1.5”).

The measurements were not fully coincidence free. The dead time was 4% for no shield and it decreased down to 1% for the maximum shield of 4.7 cm. There are two types of coincidences: true and random.

The true coincidence phenomenon does not depend on the count rate but the spectrum is changed for different shields and this may have an impact on coincidences. In particular, the low energy photons (80 keV) are heavily attenuated as a function of shield thickness. However, the true coincidence is hardly a dominating phenomenon at a source-detector distance of 100 cm. The reason is that the efficiencies are very low (< 1E-4).

Random coincidence may play a crucial role in the present experiments. It is not clear how the pileup rejector of the digital MCA (Osprey, Canberra) works. But anyway, there are much more pulse rejections at Fe thickness of 0 cm as compared with the presence of the shields.

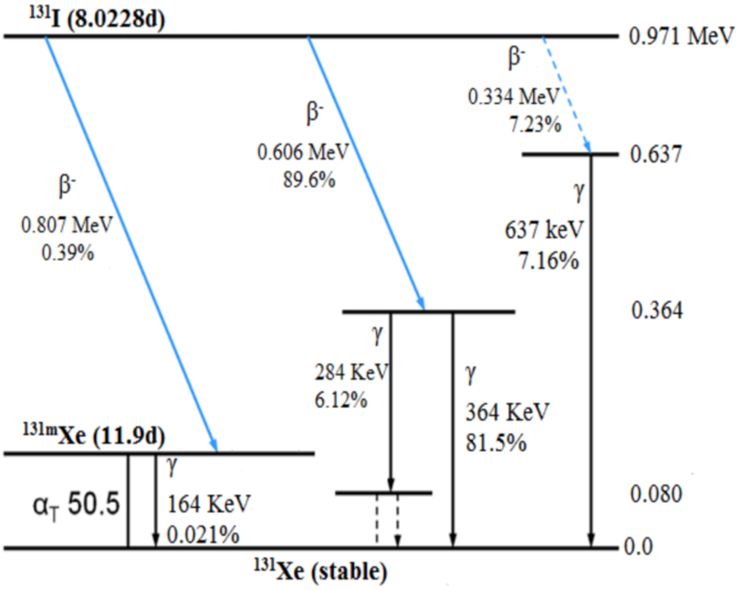

	Energy	Yield (%)
1	364.5	81.2
2	637.0	7.12
3	284.3	6.14
4	80.2	2.61

Figure 1 ***Simplified decay scheme of ^{131}I for the main emission lines. The lines 1 and 2 are coincidence free whereas line 3 is in coincidence with line 4 causing two kinds of summation: (a) "summation in" increasing peak area at 364 keV and (b) "summation out" decreasing peak area at 284 keV.***

Results

The results are shown in Figure 2. A clear conclusion is that the use of attenuation coefficients (μ_{tot}-μ_{coh}) is justified in the shield analysis. The prediction is perfect in cases (a) and (b).

The measured data points behave in somewhat strange manner (Figure 2 c). The peak area ratio does not increase at all between 0 and 0.4 cm. It should, by definition. The counting statistics do not explain the erroneous behavior. The reason may be the coincidence summation which has a different effect on different peaks. It is fully probable that the only erroneous point is the first one (0, 1) which was used to normalize the other data points. If this normalizing factor is too high then all the other data points are at level which is too low by the same factor.

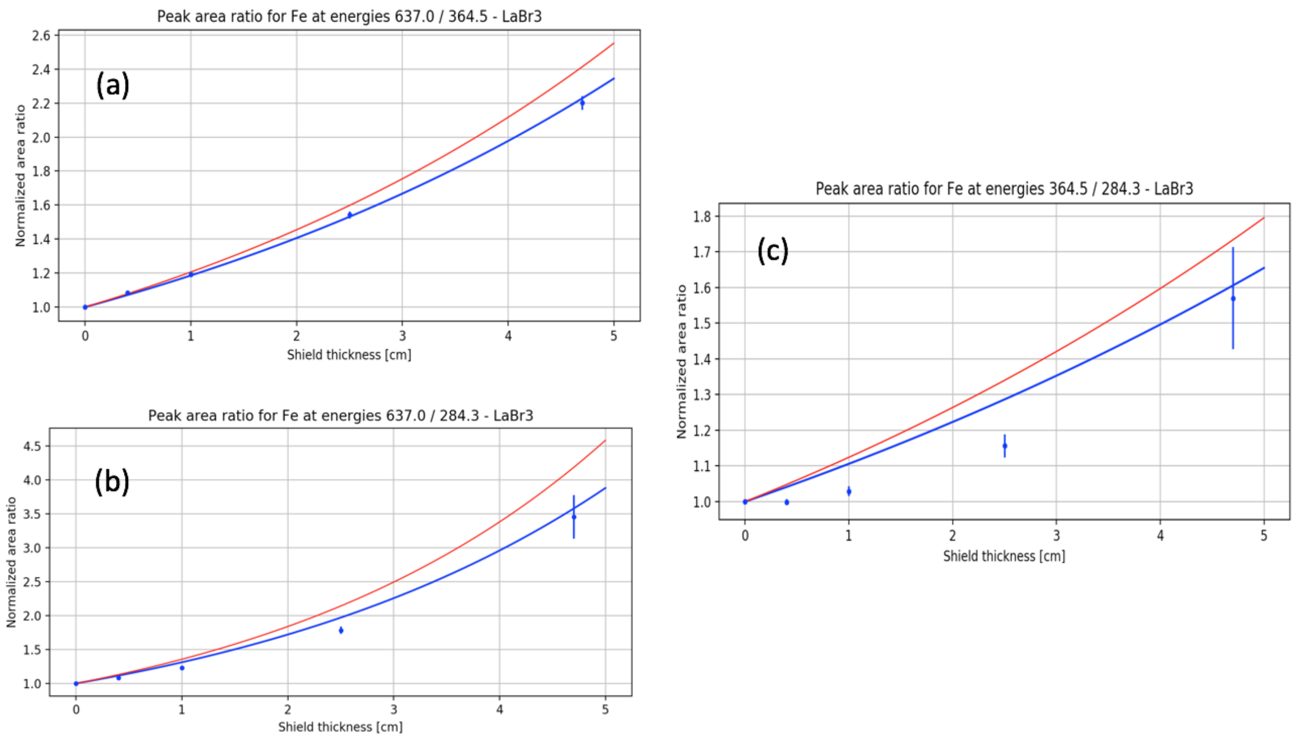

Figure 2 ***Peak area ratio in iron. The data and the curves are normalized to 1 at thickness zero. The uncertainty of the data points refers to one sigma statistics (k=1). RED curve: μ_{tot} in calculations; BLUE curve: μ_{coh} in calculations.***

Appendix 5 Source localization and estimation of source-detector distance

NKS RadShield2 measurement campaign

Umeå, 22-23 Aug 2018

Harri Toivonen, HT Nuclear

Mikko Kilkki, Environics

Sakari Ihantola, Radis Technologies

Abstract

The performance of a source localizer, RanidSOLO, was tested in field conditions. The device gave directional angles with typical accuracy of 7 - 10 degrees. The source-detector distance could be estimated with an uncertainty of 10 – 25%. This can be essentially improved by developing robust procedures to align the localizer consistently, i.e. adjusting the reference direction to north more accurately in different measurement positions. The internal directional precision of RanidSOLO is about 2 – 3%.

Source localization based on triangulation

Anti-collimation is the localization principle of RanidSOLO. The instrument is a $LaBr_3$ spectrometer surrounded with a rotating attenuator, which provides the direction of the source through reduced count rate when the attenuator is pointing towards the source. The localization method is fully automated and can achieve a high precision (a few degrees) relative to the reference direction embedded in the device. When using a digital compass to determine the reference angle, absolute directions become available. The user interface is implemented via a cell phone.

For source localization, including source-detector distance estimation, two RanidSOLO directional vectors have to be measured at different locations. When RanidSOLO reference direction is aligned with a baseline in both locations, the source-detector distance (AS and BS) can be determined with high precision even if there would be asymmetrical attenuation of photons around the source. The measurement geometry is given in Figure 1.

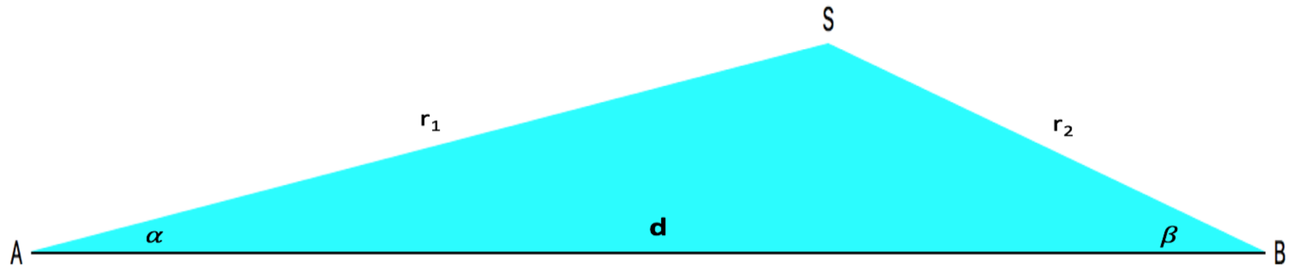

Figure 1 Triangulation for source-detector distance.

The source-detector distance AS (r_1) is

$$r_1 = d\frac{sin(\beta)}{sin(\gamma)}; \quad \gamma = \pi - \alpha - \beta \tag{1}$$

Similar expression holds for BS (swap α and β).

The uncertainty analysis is of importance for the precision of the localization and for the subsequent activity calculation. The error propagation principle provides the following estimate for the relative uncertainty of the source-detector distance:

$$\left|\frac{\Delta r_1}{r_1}\right|^2 = +\left|\frac{\Delta r_1}{r_1}\right|_d^2 + \left|\frac{\Delta r_1}{r_1}\right|_\alpha^2 + \left|\frac{\Delta r_1}{r_1}\right|_\beta^2 \tag{2}$$

where the first component of uncertainty, referring to distance *d*, is nearly zero if it can be measured accurately (laser). On the other hand, the estimation of *d* may be based on GPS coordinates with typical absolute uncertainty of $\Delta r \approx 1$ m. In some cases, the coordinates can be read from a digital map and then the user must provide not only *d* but also its uncertainty estimate. The uncertainty components are

$$\left|\frac{\Delta r_1}{r_1}\right|_d = \frac{\Delta d}{d} \tag{3}$$

$$\left|\frac{\Delta r_1}{r_1}\right|_\alpha = \frac{\Delta\alpha}{tan(\alpha)} \tag{4}$$

and

$$\left|\frac{\Delta r_1}{r_1}\right|_\beta = \left[\frac{1}{tan(\beta)} + \frac{1}{tan(\gamma)}\right] \Delta\beta. \quad (5)$$

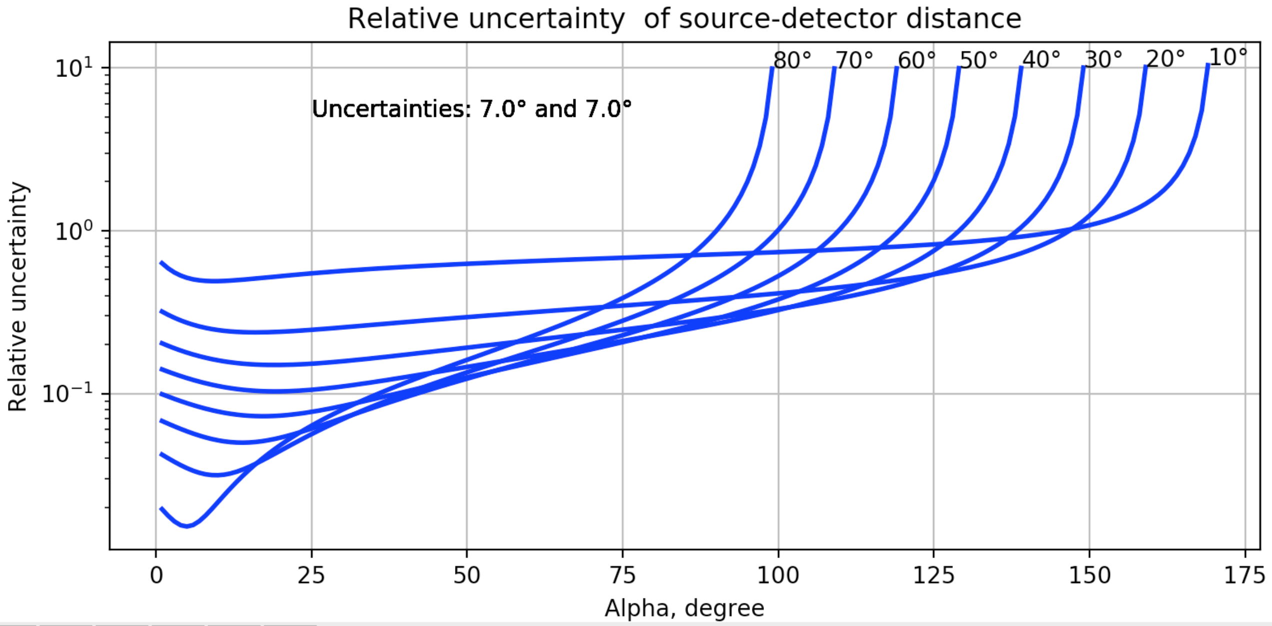

Figure 1 ***Relative uncertainty of source-detector distance. The calculation is based on Equation (2) ignoring the uncertainty related to the distance d between the two measurement points. The parameter in the upper corner is the angle β; a typical uncertainty of 7 degrees is selected for α and β.***

Figure 1 shows that the shape of the measurement triangle is very important for reducing the uncertainty. Small α and β are a very bad selection for the measurements. In this case the measurement positions and the source are almost on the same line (cps values could be used for distance estimation, see appendix 6). The triangulation works well if α is between 25 – 50 degrees and β between 30 – 80 degrees.

Source localization experiments on the FOI premises

The triangulation method described above could be operationally challenging because the distance AB has to be measured and RanidSOLO aligned according to this line. However, inside a building this may be the preferred approach.

If the map coordinates are available, then it is efficient to measure all angles relative to the magnetic north. The magnetic declination has to be included in the calculations; in Umeå it was at time of the experiments 8.12 degrees EST (positive).

The experimental results below were achieved relative to the magnetic north. RanidSOLO provided gps coordinates, directional angle towards the source and cps values for the energy interval of interest. The embedded software created XML interface files which were then processed with dedicated python scripts (*.kml output). Each measurement lasted typically 2 - 4 min.

Figure 2 ***^{137}Cs source (1.7 GBq) localized using three measurements (FHL). (a) The analyzed point of location (S) is 3.1 m from the true source location labelled as ^{137}Cs. For reference, the length of the yellow line is 10 m. The mean-deviation circle has a radius of 2.4 m. (b) Original RanidSOLO localization vectors.***

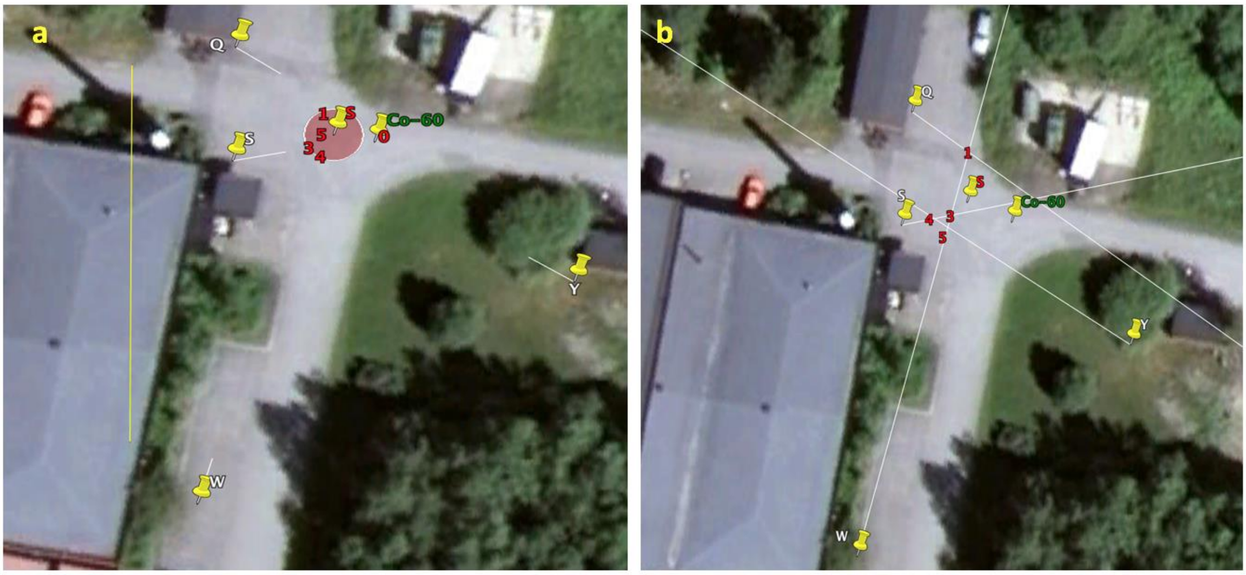

Figure 3 ***^{60}Co source (4.3 GBq) localized by four measurements (QSYW). (a) The analyzed point of location (S) is 3.8 m from the true source location labelled as ^{60}Co. For reference, the length of the yellow line is 40 m. The longest source-detector distance is 41.2 m (WS) and the mean-deviation circle has a radius of 2.6 m. (b) Original RanidSOLO localization vectors.***

The localization experiments gave a relative uncertainty of 10 – 25% for the source-detector distances (Figures 2 and 3). This same uncertainty is propagated to the activity calculation.

The present software of the RanidSOLO is designed for short term measurements. In the measurement campaign, the magnetic north was roughly determined with an auxiliary analog compass. This gave systematic errors of the order of 5 - 10%. Therefore, essential improvement in source localization accuracy can be achieved by more robust procedures to align the device exactly the same way in different measurement points. The internal directional precision of RanidSOLO is about 2 – 3%.

Appendix 6 Source localization using cps at three locations

NKS RadShield2 measurement campaign

Umeå, 22-23 Aug 2018

Gísli Jónsson, IRSA

Marjan Ilkov, IRSA

Harri Toivonen, HT Nuclear

Abstract

The peak cps values change as a function of distance ($1/r^2$). Additional decrease is due to the attenuation of photons in air, and in any shield between the source and the detector. The present study aims at studying whether these basic facts could be used to calculate the position of an unknown source. The study is restricted to an open source, i.e. no shield around the source. In fact, the thickness of the shield does not play a role if it is uniform, but it does, if the shielding is uneven to different directions. Two cps values define a circle where the source could be located. Three measurements give enough information for the source localization. The measurement campaign showed that the method works in principle. However, much more work is required to develop an operational system with iterative possibilities to analyze the attenuation of photons in air and in the unknown shielding.

Measurements and data analysis

A measurement system called SPARCS was used. The system consists of two 2 L NaI detectors, GPS antenna and acquisition unit connected to a laptop with a special GIS software. The detection system was placed in the trunk of a car so it could be driven to the measurement location swiftly. The trunk was open all the time so as not to shield the source. The sources (^{137} Cs and ^{60}Co) were placed in 15cm and 152 cm height above ground. The asphalt road provided a smooth geometry between the source and the detector; the measurements were made with a clear line of sight. Each measurement took 2-5 minutes. The GPS signal was not corrected with DGPS and some drift was in the position during each measurement. An average position was calculated for each measurement. Uncertainty in the measurement coordinates has an influence on the localization accuracy. However, for large distances, > 20 m, it is not a dominating factor. The uncertainty analysis is out of the scope of the present study.

When an unknown source is measured in two locations, the cps ratio of the peaks in the spectra form a circle where the source could be located. Three measurements are enough for source localization.

Results

Detailed analysis was performed for the ^{137} Cs source at a height of 152 cm (Table 1). The results are shown Figures 1 and 2. In this case, the locations of the measurement points were optimal for the source localization. The analysis indicates two possible solutions (symmetry); the other one has to be excluded by common sense.

Within the NKS project framework it was not possible to perform full analysis of all measurements, including uncertainty analysis. Nevertheless, the results clearly show that it is possible to develop a localization system based on the cps ratios at different measurement locations. From these first results there is long way towards the operational usage because iterative analysis methods have to be developed for photon absorption in the air and in the unknown shield which may be different to different directions.

Table 1 ***^{137}Cs source localization based on cps ratios.***

Date: 23/08/2018

Start Time	End Time	LATITUDE	LONGITUDE	Distance from source [m]
8.16.38	8.18.01	63,849639	20,334664	32,9 (D)
8.20.32	8.23.03	63,850027	20,33381	51,2 (F)
8.29.17	8.30.37	63,84994	20,335326	22,9 (H)

Figure 1 ***^{137}Cs source localization based on cps-ratios. Air absorption correction was performed iteratively by hand calculations. Difference between true and estimated location is 6.9 m.***

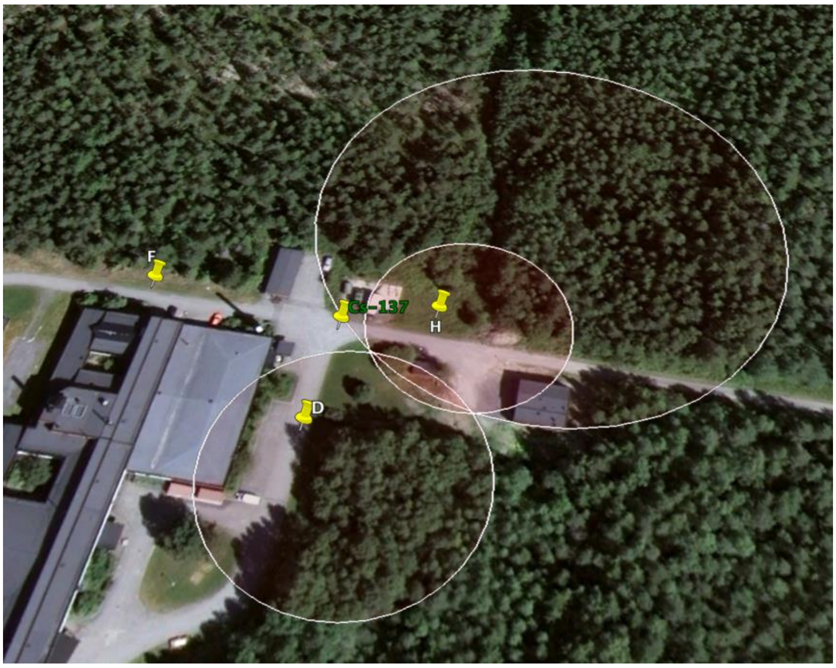

Figure 2 ***^{137}Cs source localization based on cps-ratios. Air absorption correction was not performed. Difference between true and estimated location is 10.8 m.***

Appendix 7 Measurement campaign in FOI, Umeå, 22-23 Aug 2018

The measurements were performed under field conditions

- large tent, 15 x 10 m^2, with a concrete floor
- outside the tent on an asphalt road

All measurements are labelled with a running number. This primary key refers explicitly to a specific measurement arrangement.

Day 1

Nuclide: Cs-137

Activity: 1.72 GBq

Coordinates: [20.33488, 63.84998] – Inside FOI tent (gps)

ID: 1 SDD: 5.0 m Height: 0.6 m Doserate: 7.4 uSv/h No shield

ID: 2 SDD: 5.0 m Height: 0.6 m Doserate: 7.4 uSv/h No shield

ID: 3 SDD: 5.0 m Height: 0.6 m Doserate: 2.0 uSv/h Pb 0.018 m

ID: 4 SDD: 5.0 m Height: 0.6 m Doserate: 1.5 uSv/h Pb 0.018 m

ID: 5 SDD: 5.0 m Height: 0.28 m Doserate: 7.0 uSv/h No shield

ID: 6 SDD: 5.0 m Height: 0.06 m Doserate: 7.0 uSv/h No shield

ID: 7 SDD: 5.0 m Height: 0.0 m Doserate: 7.0 uSv/h No shield

ID: 8 SDD: 5.0 m Height: 2.08 m Doserate: 6.8 uSv/h No shield

Nuclide: Co-60

Activity: 4.31 GBq

Coordinates: [20.33508, 63.85000] – Inside FOI tent (gps)

ID:10 SDD: 10.0 m Height: 0.28 m Doserate: 20.0 uSv/h No shield

ID:11 SDD: 10.0 m Height: 0.6 m Doserate: 20.0 uSv/h No shield

ID:12 SDD: 10.0 m Height: 0.06 m Doserate: 20.0 uSv/h No shield

ID:13 SDD: 10.0 m Height: 0.0 m Doserate: 20.0 uSv/h No shield

ID:14 SDD: 10.0 m Height: 2.08 m Doserate: 20.0 uSv/h No shield

Day-2

Nuclide: I-131

Activity: 0.08 GBq

Coordinates: [20.33508, 63.85000] – Inside FOI tent (gps)

ID:21 SDD: 1.0 m Height: 0.95 m Doserate: 5.0 uSv/h Fe 0.0 m

ID:22 SDD: 1.0 m Height: 0.95 m Doserate: 3.5 uSv/h Fe 0.004 m

ID:23 SDD: 1.0 m Height: 0.95 m Doserate: 2.3 uSv/h Fe 0.01 m

ID:24 SDD: 1.0 m Height: 0.95 m Doserate: 1.1 uSv/h Fe 0.025 m

ID:25 SDD: 1.0 m Height: 0.95 m Doserate: 0.6 uSv/h Fe 0.047 m

Nuclide: Cs-137

Activity: 1.72 GBq

Coordinates: [20.334814, 63.849907] – Outside FOI tent (reviewed)

ID:30 Height: 0.15 m No shield

ID:31 Height: 1.52 m No shield

Nuclide: Co-60

Activity: 4.31 GBq

Coordinates: [20.334814, 63.849907] – Outside FOI tent (reviewed)

ID:32 Height: 1.5 m No shield

ID:32 Height: 0.15 m No shield

Bibliographic Data Sheet **NKS-414**

Title	Activity estimation of shielded or hidden radionuclides in emergency conditions: Impact of environmental conditions
Author(s)	[1]H. Toivonen, [2]H. Ramebäck, [2]M. Granström, [1]S. Ihantola, [3]G. Jónsson, [3]M. Ilkov, [4]M. Kilkki
Affiliation(s)	[1]HT Nuclear, Finland [2]FOI, Sweden [3]IRSA, Iceland [4]Environics, Finland
ISBN	978-87-7893-503-8
Date	December 2018
Project	NKS-B / RadShield
No. of pages	49
No. of tables	2
No. of illustrations	28
No. of references	3

Abstract
max. 2000 characters

In 2017 an NKS project focused on the shield analysis, which showed that the spectrum contains enough information to determine the attenuation of the photons in a material between the source and the detector. Two approaches were studied: the step ratio- and the peak ratio methods. In the step ratio method, the height of the step just below a full energy peak originates from photon scattering to small angles, primarily from scattering in a shield. Using that information, the ratio of the step divided by the net area of the peak, is a function of the shield thickness. If a calibration is done with different thicknesses, that calibration can be used to determine the shield thickness. Moreover, with knowledge of the distance between the detector and the source and the efficiency of the detector at a reference distance, the activity of the source can be determined. The other approach, the peak ratio method, can be used for radionuclides emitting more than one gamma photon having enough difference in energies in its decay. That method uses the fact that the attenuation of the two gamma rays will be different. Again, knowledge of the distance and the efficiency of the detector gives the source activity.

The study in 2017 showed the effect of the environment on the shield analysis for the step ratio method when the information in the step just below a peak is to be used for the analysis. The present study focuses on the impact of the environment for this method. In particular, material other than the shield, including the ground, contributes to the small angle scattering and therefore to the step underneath the peaks. Such contributions will cause a bias in the method which has to be accounted for in the uncertainty calculation.

Another problem correlated to the uncertainty estimation is the fact that the activity of a shielded source is not linear with respect to some input quantities. If the uncertainty of those input quantities is large, normal uncertainty propagation will result in bad estimates for the uncertainty. One solution to this problem is to apply a Monte Carlo method, i.e. propagate the distributions. This was also done for the activity estimations in this work.

Key words

Gamma spectrometry, radioactive sources, activity determination, shielded sources, nuclear security

Available on request from the NKS Secretariat, P.O.Box 49, DK-4000 Roskilde, Denmark.
Phone (+45) 4677 4041, e-mail nks@nks.org, www.nks.org